Infectious stability against high temperatures and strain-dependent pathogenicity in a mouse model of severe fever with thrombocytopenia syndrome virus

重症熱性血小板減少症候群ウイルスの高温耐性とマウスモデルにおけるウイルス株による病原性の解析

Joint Graduate School of Veterinary Medicine

Yamaguchi University

Samuel NYAMPONG

September, 2026

Infectious stability against high temperatures and strain-dependent pathogenicity in a mouse model of severe fever with thrombocytopenia syndrome virus

重症熱性血小板減少症候群ウイルスの高温耐性とマウスモデルにおけるウイルス株による病原性の解析

ACADEMIC DISSERTATION

Presented to

Joint Graduate School of Veterinary Medicine

Yamaguchi University, Japan

By

Samuel Nyampong

Laboratory of Veterinary Microbiology

Joint Faculty of Veterinary Medicine,

Yamaguchi University, Japan

In partial fulfillment of the requirements for the degree of

Doctor of Philosophy (PhD)

In

Veterinary Science

September, 2026

Table of Contents

Title I
Table of Contents II
List of Tables IV
List of Figures V
Abbreviations / Definitions VI
1. 0 General Introduction 1
1.1 The Emergence of SFTSV as a Global Health Threat 2
1.2 Virology of SFTSV 2
1.2.1 Genome Organization and Structural Proteins 2
1.2.2 Interaction Between the Viral NSs Protein and Interferon 3
1.2.3 Replication of SFTSV in Mammalian Cell Lines 3
1.3 Host Immune Response and Pathogenesis 4
1.3.1 Pathogenesis: The Cytokine Storm 4
1.3.2 Animal Models of SFTSV Infection 5
1.4 Genetic Diversity and the Role of Amino Acid Substitutions 5
1.5 The Aim of This Study 6
Chapter 1: Temperature-Dependent Infectious Stability of Severe Fever with Thrombocytopenia Syndrome Virus 8
2.1 Abstract 9
2.2 Introduction 10
2.3.0 Materials and Methods 11
2.3.1 Cells and Viruses 11
2.3.2 Focus Forming Assay (FFA) 11
2.3.3 Plaque Forming Assay (PFA) 12
2.3.4 Mice Experiments 12
2.3.5 Virus Incubation at Different Temperatures 12
2.3.6 Inactivation of SFTSV by Ethanol and Sodium Hypochlorite 12
2.3.7 UV Irradiation of SFTSV 13
2.4.0 Results 14
2.4.1 Infectious Stability of SFTSV, KMV, JEV, and FCV at 4°C, 23°C, and 37°C 14
2.4.2 Infectious Stability of SFTSV, KMV, JEV, and FCV at 56°C and 94°C 16

2.4.3 Infectious Stability of SFTSV-Infected Mice Blood at 4°C, 23°C, 37°C, 56°C and 94°C 17
2.4.4 Virucidal Efficacy of Ethanol and Sodium Hypochlorite on SFTSV Infectivity 18
2.4.5 Inactivation Efficacy of UV Irradiation on SFTSV Infectivity 19
2.5 Discussion 21
2.6 Conclusion 24
Chapter 2: Comparison of Pathogenicity in IFN-I Interferon Receptor-Deficient A129 Mice and Characterization of Amino Acid Substitutions among Severe Fever with Thrombocytopenia Syndrome Virus Strains 25
3.1 Abstract 26
3.2 Introduction 27
3.3.0 Materials and Methods 29
3.3.1 Viruses and Cells 29
3.3.2 Focus Forming Assay (FFA) 29
3.3.3 SFTSV Infection in Mice 29
3.3.4 Quantification of Viral RNA 30
3.3.5 Viral Genome Sequencing and Phylogenetic Analysis 30
3.3.6 Virus Growth Kinetics 31
3.3.7 Statistical Analysis 31
3.4.0 RESULTS 32
3.4.1 The Pathogenicity of SFTSV Strains in Infected Cats and A129 Mice 32
3.4.2 Viral Loads in Organs of SFTSV-infected Mice with Fatality Rates of 20-100% 33
3.4.3 Amino Acid Substitutions of the Other SFTSV Strains Relative to TK-F123 34
3.4.4 Growth Kinetics in VeroE6 and TLT Cell Lines 38
3.4.5 Phylogenetic Analysis of the SFTSV Strains used In This study 39
3.5.0 Discussion 42
3.6 Conclusion 44
4.0 General Conclusion 45
Acknowledgment 46
References 47

List of Tables

Table Number	Table Title	Page Number
Table 3.1	Cat-derived SFTSV strains used in this study	**30**
Table 3.2	Amino-acid substitutions among SFTSV strains relative to the SFTSV Tk-F123 strain	**33-34**

List of Figures

Figure Numbers	Figure Tittle	Page Numbers
Figure 2.1	Viral infectious titers of SFTSV, KMV, JEV, and FCV after incubation at 4℃, 23℃, and 37℃	**15**
Figure 2.2	Viral infectious titers of SFTSV, KMV, JEV, and FCV after incubation at 56℃ and 94℃.	**16**
Figure 2.3	Log-reduction of SFTSV infectivity in blood across varying temperatures.	**17**
Figure 2.4	Viral infectious titers of SFTSV after treatment with 70% ethanol and 1% sodium hypochlorite	**18**
Figure 2.5	Inactivation rates of SFTSV by UV light	**19**
Figure 3.1 (A)	Pathogenicity of cat-derived SFTSV strains in IFNAR-deficient A129 mice	**31**
Figure 3.1 (B)	Viral RNA copy numbers in tissues from mice infected with SFTSV strains Tk-F123, Ng-F125, Ng-F265, Yg-F197, and Ng-F264	**32**
Figure 3.2	Growth kinetics of SFTSV strains	**36**
Figure 3.3	Phylogenetic trees based on the full-length nucleotide sequences of the SFTSV strains S, M, and L segments	**37**

Abbreviations / Definitions

Abbreviation	Definition
Ala	Alanine
Arg	Arginine
Asn	Asparagine
Asp	Aspartic acid
BHK-21	Baby-Hamster Kidney
BSL	Biosafety level
CCHFV	Crimean-Congo hemorrhagic fever virus
CPE	Cytopathic effect
CRFK	Crandel-Feline Ress kidney
cRNA	Complementary RNA
DC-SIGN	Dendritic-cell-specific intracellular adhesion molecule-3-grabbing non-integrin
DIC	Disseminated intravascular coagulation
DMEM	Dulbecco Modified Eagle's Medium
DUV-LED	Deep-ultraviolet light-emitting diode
FCV	Feline calicivirus
FFA	Focus-forming assay
Gc	Glycoprotein c
Gln	Glutamine
Glu	Glutamic acid
Gly	Glycine
Gn	Glycoprotein n
GPC	Glycoprotein precursors
His	Histidine
HNTV	Hantaan virus

IB	Inclusion bodies
IFNAR	Type-I Interferon-receptor
IFNAR $^{-/-}$	Type-I interferon receptor knockout
IFNAR1	Interferon Alpha/Beta Receptor Subunit 1
IFN-I	Type-I interferon
IFNs	Interferons
IFN-γ	Interferon gamma
IKKε	Inhibitor of κB kinase epsilon
IL	Interleukin
Ile	Isoleucine
IP-10	Interferon gamma–inducible protein 10
IRF3	Interferon Regulatory Factor 3
JEV	Japanese encephalitis virus
KAMV	Kabuto mountain virus
Leu	Leucine
LOD	Limit of detection
Lys	Lysine
MCP-1	Monocyte Chemoattractant Protein-1
Met	Methionine
MODs	Multiple organ dysfunction
MOI	Multiplicity of infection
N	Nucleocapsid protein
NSs	Non-structural S protein
PFA	Plaque-forming assay
Phe	Phenylalanine
Pro	Proline
PRRS	Pattern Recognition Receptors
RdRp	RNA-dependent RNA polymerase
RIG-I	Retinoic acid-Inducible Gene I

RNP	Ribonucleoprotein complex
RVFV	Rift Valley fever virus
Ser	Serine
SFTS	Severe fever with thrombocytopenia syndrome
SFTSV	Severe fever with thrombocytopenia syndrome virus
STAT2	Signal transducer and activator of transcription 2
TBK1	TANK-Binding Kinase 1
Thr	Threonine
TLT	Tiger liver tumor
TNF-α	Tumor Necrosis Factor-alpha
Trp	Tryptophan
Tyr	Tyrosine
UV-CCl	Ultraviolet-C cold-cathode lamp
Val	Valine
VE6	Vero E6
vRNA	Viral RNA

1. 0 General Introduction

1.1 The Emergence of SFTSV as a Global Health Threat

In recent years, emerging and re-emerging infectious diseases have not only persisted but also appeared in new and unpredictable ways. Zoonotic RNA viruses are no exception and pose a particularly formidable threat to public health (Jones et al., 2008). Climate change, agricultural intensification, increased human mobility, and greater human-animal interactions are key drivers of pathogen spillover from wildlife and arthropod vectors into the human population (Morens et al., 2004). Among these emerging threats, tick-borne viruses have gained significant notoriety, exemplified by the discovery of the Severe Fever with Thrombocytopenia Syndrome Virus (SFTSV).

SFTSV was first identified in rural areas of the Hubei and Henan provinces in China, following investigations into an unexplained febrile illness characterized by thrombocytopenia, leukopenia, and high mortality (Yu et al., 2011). Initial genomic analysis revealed a novel virus, which was subsequently classified as a member of the genus Bandavirus within the family Phenuiviridae and the order Bunyavirales (Yu et al., 2011).

Since its discovery, SFTS has proven to be a significant and expanding public health burden across East Asia. While China remains the most heavily endemic region, the virus has also been reported as endemic in South Korea and Japan and has more recently been detected in Vietnam and Taiwan (Kim et al., 2013; Takahashi et al., 2014; Tran et al., 2019; Lin et al., 2020). SFTSV is primarily transmitted by the tick vector *Haemaphysalis longicornis* (Zhang et al., 2011). The clinical spectrum of SFTSV infection ranges from mild, self-limiting febrile illness to severe hemorrhagic fever with multi-organ dysfunction syndrome (MODS) and a staggering case fatality rate that can approach 30% in humans, underscoring its clinical significance (Gai et al., 2012; Liu et al., 2014; Li et al., 2024; Kim et al., 2018). In light of the substantial disease burden and the absence of effective vaccines or treatments, the World Health Organization has designated SFTSV as a high-priority pathogen for research and development to improve therapeutic options (World Health Organization, 2018).

1.2 Virology of SFTSV

1.2.1 Genome Organization and Structural Proteins

SFTSV is an enveloped virus with a tripartite, single-stranded, negative-sense RNA genome comprising the Large (L), Medium (M), and Small (S) segments (Yu et al., 2011). The L-segment (~6.4kb) encodes the viral RNA-dependent RNA polymerase (RdRp), an enzyme critical for viral genome replication and transcription (Brennan et al., 2015; Lei et al., 2015; Reguera et al., 2016). The M segment (~3.4kb) encodes a single glycoprotein precursor (GPC), which is post-

translationally cleaved by host proteases into two surface glycoproteins, Gn and Gc (Lei et al., 2015; Brennan et al., 2015; Yu et al., 2011). These glycoproteins form heterodimeric spikes on the virion surface. The Gc subunit contains a class II fusion loop, while Gn likely shields the fusion loop in the prefusion state (Halldorsson et al., 2018). The SFTSV envelope glycoproteins Gn and Gc mediate host-cell attachment and low-pH-dependent membrane fusion during endosomal entry. They are the major targets of virus-neutralizing antibodies. (Hofmann et al., 2013; Kim et al., 2019). The S-segment, using an ambisense coding strategy, encodes the nucleocapsid protein (N) and the non-structural protein (NSs). The N protein encapsidates the viral RNA to form the ribonucleoprotein (RNP) complex, which is essential for viral transcription and replication (Yu et al., 2011; Zhou et al., 2013; Lokupathirage et al., 2021).

1.2.2 Interaction Between the Viral NSs Protein and Interferon

The non-structural protein is a major virulence factor of SFTSV, functioning as a potent type-I interferon (IFN-1) antagonist (Wu et al., 2014). Interferons are cytokines that bridge innate and adaptive immunity and are classified into type-I IFNs (IFN-alpha/beta), type-II (IFN-gamma), and type-III (IFN-lambda) (Kopitar-Jerala, 2017; Dalskov et al., 2023). Interferons (IFNs) represent the first line of defense against viral pathogens (Kopitar-Jerala, 2017; Dalskov et al., 2023). The induction of IFN-1 is a cornerstone of the host's antiviral defense, activating a signaling cascade through pattern recognition receptors (PRRs) such as Retinoic-acid Inducible Gene 1 (RIG-I), which subsequently activates the kinases TANK-Binding Kinase 1 (TBK1) and Inhibitor of κB kinase epsilon (IKKε) (Brisse & Ly, 2019). SFTSV's NSs, however, actively subvert this pathway by forming characteristic cytoplasmic inclusion bodies (IBs). It sequesters key host proteins and factors within these IBs, thereby isolating them and blocking their functions, paving the way for unchecked viral replication (Wu et al., 2014; Ning et al., 2015; Lee & Shin, 2021). Furthermore, NSs has been reported to inhibit the host gene transcription machinery and disrupt signal transducer and activator of transcription 2 (STAT2)-mediated interferon signaling, thereby crippling the IFN response (Yoshikawa et al., 2019, 2023). This potent IFN-antagonist activity is central to SFTSV pathogenesis, and NSs dysfunction results in marked attenuation (Bryden et al., 2022).

1.2.3 Replication of SFTSV in Mammalian Cell Lines

SFTSV infection begins when virus particles attach to host cell surface receptors. Among these, the C-type lectin DC-SIGN has been identified as an important entry receptor, and the viral glycoproteins Gn/Gc mediate pH-dependent, cathepsin-mediated endocytosis (Hofmann et al., 2013). Following internalization, the acidic endosomal environment triggers a conformational rearrangement of the Gc glycoprotein, enabling fusion of the viral envelope with the endosomal membrane and the release of RNP complexes into the cytoplasm. (Halldorsson et al., 2016). As a negative-sense RNA virus,

SFTSV relies on its L protein, which possesses RdRp activity, to carry out transcription of viral mRNAs and replication of the genomic RNA. During genome replication, the negative-sense viral RNA (vRNA) is first copied into positive-sense complementary RNA (cRNA), which then serves as a template for the production of progeny vRNA. These processes take place within specialized cytoplasmic replication compartments (Reguera et al., 2016; Brennan et al., 2015). The ambisense coding strategy of the S segment directs the production of both the N protein, which encapsidates nascent vRNA, and the NSs. The NSs protein rapidly forms cytoplasmic IBs that sequester key signaling molecules, including TBK1 and IKKε, thereby blocking interferon regulatory factor 3 (IRF3) phosphorylation and suppressing the induction of IFN-I responses. (Ning et al., 2014; Wu et al., 2014). The M segment encodes the GPC that is translated in the endoplasmic reticulum, glycosylated, and cleaved into the mature glycoproteins Gn and Gc. (Plegge et al., 2016). These proteins then traffic to the Golgi apparatus, where virion assembly takes place (Lundu et al., 2018). Mature virions form when RNPs bud into Gn/Gc-containing membranes of the Golgi and are then transported to the plasma membrane within secretory vesicles. Finally, progeny virions are released from the cell via exocytosis, enabling spread to neighboring cells and systemic dissemination within the host. (Overby et al., 2007; Elliott, 2014; Yan et al., 2022)

1.3 Host Immune Response and Pathogenesis

1.3.1 Pathogenesis: The Cytokine Storm

Severe SFTS is characterized by a profoundly dysregulated host immune response, commonly referred to as a cytokine storm. Clinical studies consistently show that fatal cases have markedly elevated serum levels of multiple pro-inflammatory cytokines and chemokines, including interleukin-6 (IL-6), interleukin-10 (IL-10), tumor necrosis factor-alpha (TNF-α), interferon gamma (IFN-γ), interferon gamma-inducible protein 10 (IP-10), and monocyte chemoattractant protein-1 (MCP-1), compared with survivors (Sun et al., 2012; Xu et al., 2024). This hypercytokinemia is strongly associated with vascular leakage, disseminated intravascular coagulation (DIC), and multi-organ failure, collectively defining the terminal pathophysiology of SFTS (Gai et al., 2012).

A key upstream driver of this dysregulated inflammatory response is the early suppression of IFN-1 signaling. SFTSV's NSs interferes with antiviral signaling by forming cytoplasmic inclusion bodies that sequester essential components of the RIG-I/TBK1/IKKε pathway, thereby delaying or preventing the induction of IFN-1 (Ning et al., 2014; Wu et al., 2014). This early IFN blockade permits uncontrolled viral replication during the initial phase of infection. As viral burden escalates, the host mounts an abrupt and overwhelming inflammatory response, culminating in the cytokine storm characteristic of severe and fatal SFTS.

1.3.2 Animal Models of SFTSV Infection

The study of SFTSV pathogenesis relies heavily on appropriate animal models. Immunocompetent mice, such as C57BL/6 and BALB/c, are largely resistant to SFTSV disease, owing to a rapid and robust IFN-1 response that suppresses viral replication before significant pathology can occur (Jin et al., 2012). To circumvent this limitation, researchers employ the A129 mouse, which carries a targeted deletion of the interferon alpha/beta receptor subunit 1 (IFNAR1) gene and therefore lacks the IFN-1 receptor ($IFNAR^{-/-}$) (Müller et al., 1994). In the absence of IFN-1 signaling, A129 mice become highly susceptible to SFTSV infection and develop a fulminant, often lethal disease that strikingly recapitulates severe human SFTS. This includes marked thrombocytopenia, leukopenia, high viral loads in blood and tissues, and pronounced elevations in pro-inflammatory cytokines (Liu Q et al., 2014; Matsuno et al., 2017). Because A129 mice recapitulate the essential clinical and immunopathological features of human SFTS, they are widely used as an established small animal model for evaluating viral virulence, testing antiviral therapeutics, and dissecting the intrinsic pathogenic potential of diverse SFTSV isolates, independent of the host's primary antiviral defense (Matsuno et al., 2017; Yoshikawa et al., 2019; Bryden et al., 2022).

1.4 Genetic Diversity and the Role of Amino Acid Substitutions

SFTSV, like other RNA viruses, exists as a heterogeneous quasispecies population generated by the intrinsically error-prone activity of its RdRp and shaped by host and environmental selective pressures (Duffy, 2018). Comparative genomic analyses of circulating SFTSV strains reveal substantial genetic diversity across all three genomic segments, with notable sequence divergence particularly in the M and S segments. Phylogenetic analyses demonstrate marked geographic structuring, with predominant lineages associated with China, Japan, and South Korea. Nevertheless, occasional cross-regional clustering and reassortment events indicate ongoing interregional transmission and viral genomic mixing (Yoshikawa et al., 2015; Lv et al., 2017; Wang et al., 2023). Although purifying selection predominates across the genome, a limited number of codon sites in the L, M, and S segments exhibit signatures of positive selection, suggesting ongoing adaptive evolution at discrete amino acid sites (Liu et al., 2016; Wang et al., 2023; Park et al., 2024).

Functional studies have begun to link specific amino acid substitutions to measurable phenotypic differences. A well-characterized example is the R962S (arginine-to-serine) substitution in the Gc glycoprotein, which modulates membrane fusion activity and is critical for viral infection. Strains carrying the Ser_{962} variant exhibited enhanced fusion activity and increased infectivity (Tani et al., 2019). More recently, two additional residues in Gc, Gly_{581} and Ser_{934} were

identified as key determinants of virulence. Experimental studies showed that the strain Tk-F123 carrying the Gly_{581}/Ser_{934} combination caused severe and lethal disease in A129 mice, whereas the Ng-F264 strain harboring the Arg_{581}/Asn_{934} variants was markedly attenuated (Wulandari et al., 2025). These findings underscore that single or paired amino acid substitutions can profoundly influence viral entry, infectivity, and in vivo pathogenicity. Despite these advances, the amino acid determinants underlying temperature-dependent stability, a phenotype central to this thesis, remain unknown. Moreover, although individual virulence-associated residues have been identified, our knowledge of systematic comparisons of pathogenicity across a panel of naturally occurring strains and of correlations between these phenotypes and specific amino acid substitutions in the $IFNAR^{-/-}$ model remains limited. Addressing this gap is essential to understanding how natural sequence variation shapes SFTSV virulence and environmental fitness.

1.5 The Aim of This Study

In the absence of vaccines or targeted therapeutics, SFTSV prevention relies on interrupting transmission pathways. Given documented incidence of animal-human and human-human transmissions, understanding viral inactivation is critical for infection control. Characterizing SFTSV's environmental persistence and inactivation conditions were investigated as a measure to mitigate infection risk. The specific aims of this study, presented in chapters 1 and 2 of this thesis, were as follows:

Chapter 1: Temperature-dependent infectious stability of SFTSV

- To evaluate the temperature-dependent infectious stability of the SFTSV at 4°C, 23°C, and 37°C, representing seasonal environmental temperatures.
- To evaluate the effect of heat (56°C and 94°C) on SFTSV infectivity.
- To assess the inactivation efficacy of 70% ethanol and 1% sodium hypochlorite against SFTSV infectivity.
- To determine the effect of ultraviolet (UV) wavelengths (254nm, 265nm, and 275 nm) on SFTSV infectivity.

Chapter 2: Comparison of pathogenicity in IFN-I receptor-deficient A129 mice and characterization of amino acid substitutions among severe fever with thrombocytopenia syndrome virus strains

- To compare the pathogenicity of 14 cat-derived SFTSV strains (isolated from naturally infected cats) in the A129 ($IFNAR^{-/-}$) mouse model.

- To quantify viral RNA loads in representative tissues, such as the liver, kidney, and brain of infected mice.
- To sequence full-length genomes and identify potential amino acid substitutions that may be associated with the observed pathogenicity.
- To characterize the growth kinetic properties of five representative strains with a fatality range of 20–100% in highly susceptible SFTSV cell lines.
- To perform phylogenetic analysis to identify the dominant genotypes circulating among the studied isolates.

Chapter 1: Temperature-Dependent Infectious Stability of Severe Fever with Thrombocytopenia Syndrome Virus

2.1 Abstract

Severe fever with thrombocytopenia syndrome virus (SFTSV) is an emerging tick-borne zoonotic pathogen of increasing concern in East Asia, including Japan. Not only humans but also domestic cats are highly susceptible and frequently develop severe disease. Despite its public and veterinary health significance, data on the environmental stability of SFTSV remain limited. In this study, we evaluated the stability profiles of SFTSV under various temperature and inactivation conditions. As comparative controls, Kabuto Mountain virus (KAMV) which belongs to the same class and order as SFTSV, Japanese Encephalitis virus (JEV) representing a different type of enveloped virus, and Feline Calicivirus (FCV) representing an example of non-enveloped virus, were also tested. SFTSV showed higher infectious stability at 4 ℃, 23 ℃ and 37 ℃ compared to KAMV, JEV and FCV. In addition, SFTSV demonstrated comparatively higher resistance to heat inactivation at 56℃ and 94℃. On the other hand, SFTSV was easily inactivated by ethanol, hypochlorite and ultraviolet irradiation. These findings provide important insights into the environmental persistence and inactivation requirements of SFTSV, suggesting that appropriate inactivation procedures are important to reduce the risk of SFTSV infection from the contaminated samples at clinical sites and laboratories.

2.2 Introduction

Severe fever with thrombocytopenia syndrome (SFTS) virus (SFTSV) is an emerging tick-borne pathogen that first emerged in China (Yu et al., 2011). Currently, it is known that SFTSV is distributed in East to Southeast Asian countries, including Japan, South Korea, Vietnam, and Taiwan (Kim et al., 2013; Takahashi et al., 2014; Tran et al., 2019; Lin et al., leukopenia, and multi-organ failure, with a fatality rate of as high as 30% (Liu Q et al., 2014; Kim et al., 2018). SFTSV is classified within the family *Phenuiviridae*, genus *Bandavirus*, and species *Bandavirus dabieense*. It is an enveloped virus with a genome composed of three RNA segments: S, M, and L (Zhang et al., 2011; Lei et al., 2015). SFTSV is transmitted by ticks such as *Haemaphysalis longicornis* and *Amblyomma testudinarium* (Zhang et al., 2011, 2012; Yun et al., 2014), and virus infections typically occur through tick bites, and human-to-human transmission from SFTS cases has also been reported (Gai et al., 2012; Fang et al., 2021).

SFTSV-antibody-positive animals have been reported, including wild boars, deer, goats, cattle, pigs, and chickens (Niu et al., 2013; Ding et al., 2014; Tabara et al., 2016). Of note, SFTS cases have been identified in cats, dogs, and cheetahs (Matsuno et al., 2018; Matsuu et al., 2019; Park et al., 2019; Sakai et al., 2021). In particular, numerous cat cases have been documented, and they appear to be highly susceptible to SFTSV infection, with mortality rates of up to 60% (Matsuu et al., 2019). Notably, infectious SFTSV and viral genomes have been detected in body fluids such as saliva, tears, and urine from SFTS cases (Yamanaka et al., 2020; Kirino et al., 2021; Tsuru et al., 2021), raising the risk of infection from animals infected with SFTSV, especially for veterinarians, veterinary nurses, and pet owners. Therefore, to reduce the risk of this zoonotic infection, implementing prevention measures is crucial in veterinary practice, including safe handling of animals, the use of personal protective equipment, and proper disinfection and sterilization. In addition, understanding the environmental stability of SFTSV and its susceptibility to inactivation is key for infection control in animal hospitals. Previous studies showed that SFTSV was stable at relatively high temperatures (Harada et al., 2020), suggesting that the infectious status of the virus may be stable at temperature-dependent conditions and resistant to heat inactivation.

In this study, we examined the infectious stability of SFTSV across a range of temperatures from as low as 4°C to as high as 94°C. Additionally, we evaluated the inactivation effects of ethanol, sodium hypochlorite and ultraviolet (UV) irradiation. Our results provide valuable information on preventive measures for SFTSV based on its temperature-dependent stability.

2.3.0 Materials and Methods

2.3.1 Cells and Viruses

SFTSV Tk-F123 strain was isolated from cat serum in Tokushima (Wulandari et al., 2025). Japanese encephalitis virus (JEV) YD-1 strain, isolated from a mosquito collected in Yamaguchi, Japan, was kindly provided by Ken Maeda of Japan Institute for Health Security (Kuwata et al., 2015). Kabuto mountain virus (KAMV) Nag strain was isolated from *Haemaphysalis flava* collected in Hirado, Nagasaki, Japan (unpublished results). Feline calicivirus (FCV) was purchased from the American Type Culture Collection. SFTSV and KAMV were propagated in Vero E6 cell lines, JEV in baby hamster kidney (BHK)-21, FCV in Crandell-Reese feline kidney (CRFK) cell lines. Supernatants from virus-infected cells were harvested after 2 days for JEV, 4 days for KAMV and FCV, and 5 days for SFTSV, prior to the appearance of significant cytopathic effects, and viral stocks were prepared. Cells were cultured in Dulbecco's Modified Eagle's Medium (DMEM) (Thermo Fisher Scientific Inc., Waltham, Massachusetts, USA) supplemented with 10% heat-inactivated fetal bovine serum (FBS) (Serena Europe GmbH, Pessin, Germany) and 1% penicillin-streptomycin (100 U/mL penicillin and 100 µg/mL streptomycin; FUJIFILM Wako Pure Chemical Corporation, Osaka, Japan), and maintained at 37°C in 5% CO_2. Experiments with infectious SFTSV were conducted in a biosafety level (BSL)-3 laboratory at Yamaguchi University, following standard BSL-3 guidelines. KAMV, JEV, and FCV experiments were carried out in a BSL-2 laboratory.

2.3.2 Focus Forming Assay (FFA)

SFTSV infectious titers were determined by FFA as previously described (Hayasaka et al., 2015). Briefly, confluent VeroE6 cells were inoculated with serially diluted culture supernatants of the SFTSV stock and incubated with overlaid 2% FBS DMEM containing 1% methylcellulose (MC) (Wako Pure Chemical Industries, Ltd., Tokyo, Japan) for 3 days. The viral foci were detected using SFTSV monoclonal antiserum, peroxidase-conjugated anti-mouse IgG (American Qualex, San Clemente, CA, USA), and DAB substrate (Wako Pure Chemical Industries, Ltd.). Viral titers were expressed as ffu/mL.

2.3.3 Plaque Forming Assay (PFA)

Infectious titers of KAMV, JEV, and FCV were measured by PFA (Hu et al., 2024). Briefly, serially diluted viruses were inoculated into each confluent cell culture and incubated for 90 min; thereafter, 1% MC DMEM was applied. Plaques were visualized with 1% crystal violet (FUJIFILM Wako Pure Chemical Corp.). Viral titers were expressed as pfu/mL.

2.3.4 Mice Experiments

IFNAR $^{-/-}$ A129 mice were purchased from B&K Universal Limited and mated at Yamaguchi University, Japan. Twenty-five mice were subcutaneously inoculated with 10^5 ffu of SFTSV. The mice were euthanized at 3 days post-infection (dpi), and blood samples were collected and pooled. The animal experiments were conducted in accordance with the Fundamental Guidelines for the Proper Conduct of Animal Experiments and Related Activities in Academic Research Institutions under the jurisdiction of the Ministry of Education, Culture, Sports, Science, and Technology. The Animal Care and Use Committee of Yamaguchi University approved all the experimental protocols (approval number: 05-31-565).

2.3.5 Virus Incubation at Different Temperatures

Each virus was diluted to 5×10^5 ffu/mL or pfu/mL in DMEM supplemented with 2% FBS, and 0.25 mL of each virus aliquot was incubated at 4°C, 23°C, 37°C, 56°C, and 94°C in polypropylene tubes. Pooled blood samples were aliquoted into 0.15 mL portions in tubes. Samples stored at 4°C, 23°C and 37°C were collected daily by 7 dpi, and those at 56°C and 94°C were collected after 1, 10, 30 and 60 min. Retrieved samples were stored at -80°C until titration. All experiments were conducted in duplicate with three independent repetitions.

2.3.6 Inactivation of SFTSV by Ethanol and Sodium Hypochlorite

Each virus was mixed with 70% ethanol (Wako Pure Chemical Industries, Ltd.) or 100 ppm sodium hypochlorite (Wish-s-SH, Chappie Co., Ltd., Yamaguchi, Japan) at the ratio of 1:9 and incubated for 1, 5, and 10 min. Retrieved samples were stored at -80°C until use, and viral titers were determined by FFA. All experiments were conducted in duplicate with three independent experiments.

2.3.7 UV Irradiation of SFTSV

UV irradiation was performed as previously described (Shimoda et al., 2021). Briefly, virus solutions were placed on a 50-mm dish (Sumitomo Bakelite Inc., Tokyo, Japan) and irradiated for 4, 8, 12 and 20 sec (254 nm UV-CCL), 7, 14, 21 and 28 sec (265 nm DUV-LED), and 15, 30, 45 and 60 sec (275 nm DUV-LED) (Stanley Electric Co., Ltd., Tokyo, Japan). UV intensity (mW/cm^2) was measured using a chemical actinometer, KI/KIO_3 (Rahn et al., 2003), and calculated with the Lambert-Beer law (Beniac et al., 2012). All experiments were performed in duplicate with three independent experiments.

2.4.0 Results

2.4.1 Infectious Stability of SFTSV, KMV, JEV, and FCV at 4°C, 23°C, and 37°C

We first examined the infectious stability of SFTSV at 4°C, 23°C, and 37°C, simulating conditions representative of temperatures throughout the year. These temperatures also represent typical refrigerator, room and incubator for cell culture, respectively. As comparative control belonging to the same class *Bunyaviricetes*, order *Harenavirals* as SFTSV, KAMV (family *Phenuiviridae*, genus *Uukuvirus*) was tested. In addition, JEV (family *Flaviviridae*, genus *Orthoflavivirus*) and FCV (family *Caliciviridae*, genus *Vesivirus*) were used as representatives of a different enveloped virus and a non-enveloped virus, respectively.

At 4°C, infectious titers of SFTSV and JEV showed almost no decrease over 7 days, while titers of KAMV and FCV decreased by 1.0 and 1.26 log10 ffu/mL (differences relative to the titers of day 0 controls) after 7 days, respectively (Figure 1). At 23°C, SFTSV experienced a slight decrease with a 1.73 log10 ffu/mL reduction after 7 days (Figure 1). JEV showed a 2.36 log10 ffu/mL reduction after 7 days (Figure 1). In contrast, KAMV and FCV markedly reduced their titers to below detection limits by 5 days and 2 days, respectively (Figure 1). At 37°C, SFTSV declined gradually, but its titer remained at 2.71 log10 ffu/mL after 7 days (Figure 1). On the other hand, infectious titers of KAMV, JEV, and FCV decreased significantly to below detection limits by 3 days, 2 days, and 1 day, respectively (Figure 1).

These observations indicate that SFTSV was remarkably stable at 4 to 37°C compared with other viruses, suggesting that SFTSV-contaminated samples may retain infectious ability in a clinical environment for a long time throughout the year. The data also provide useful information indicating that SFTSV samples can be stored at 4°C without a significant reduction of infectious titers for diagnosis by viral detection.

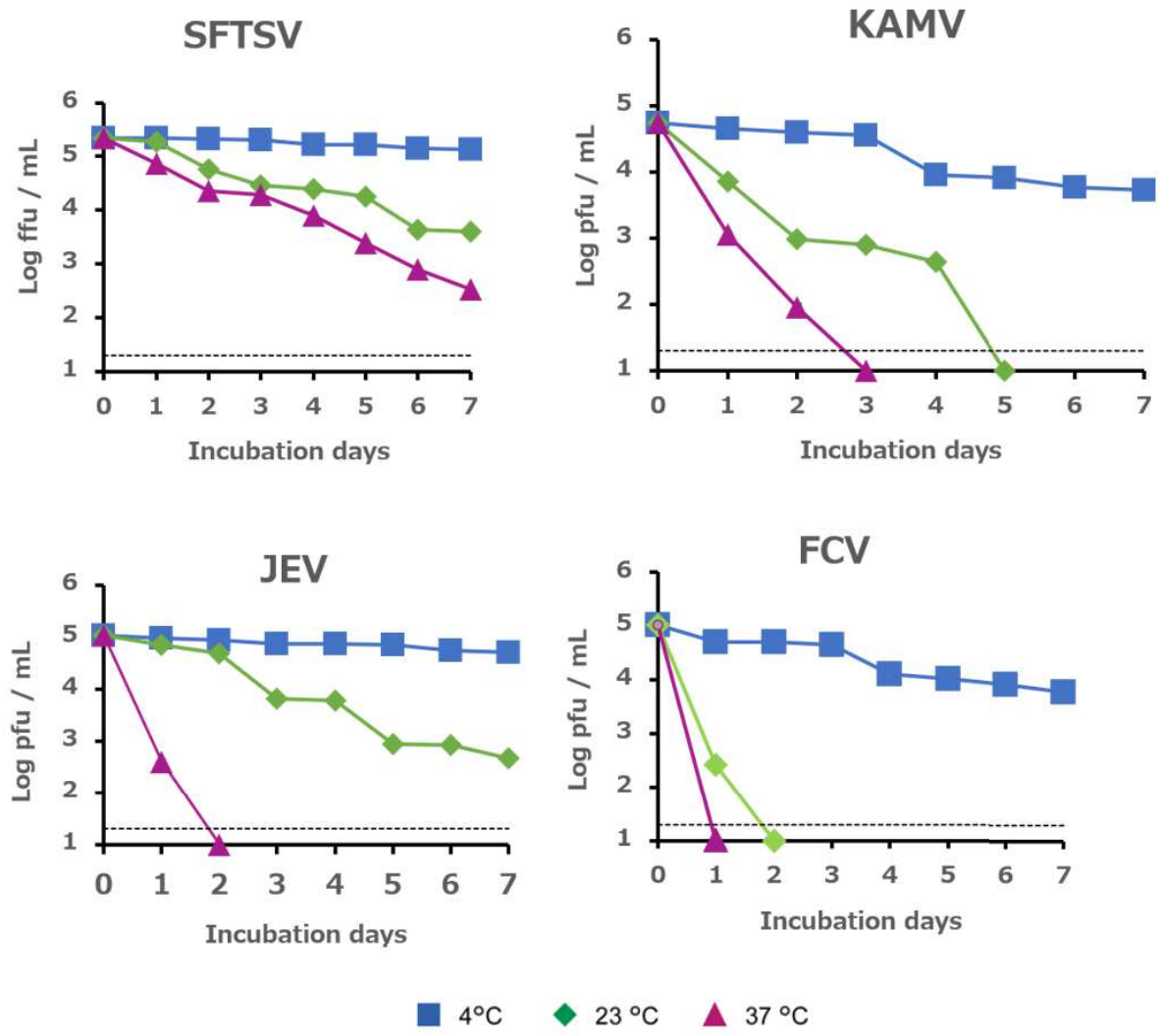


Fig. 2.1 Viral infectious titers of Severe fever with thrombocytopenia syndrome virus (SFTSV), Kabuto Mountain virus (KMV), Japanese Encephalitis virus (JEV), and Feline Calicivirus (FCV) after incubation at 4°C, 23°C, and 37°C. Approximately 1.25×10^5 ffu/mL of each virus in 0.25 mL of 2% FCS MEM were incubated at these temperatures, with samples collected daily. Viral titers were measured as ffu/mL (SFTSV) or pfu/mL (KAMV, JEV, FCV). Control viral titers (day 0) were $10^{5.34}$ ffu/mL (SFTSV), $10^{4.74}$ pfu/mL (KAMV), $10^{5.03}$ pfu/mL (JEV), and $10^{5.03}$ pfu/mL (FCV). Each data point was obtained from three independent experiments at the indicated time points. Error bars represent standard errors. The dotted line indicates the detection limit of SFTSV ($10^{1.3}$ ffu/mL).

2.4.2 Infectious Stability of SFTSV, KMV, JEV, and FCV at 56°C and 94°C

We next evaluated the heat stability of SFTSV at 56°C and 94°C, simulating typical serum complement inactivation and near-boiling temperature, respectively. Interestingly, infectious SFTSV remained at 56°C with a 2.32 log10 ffu/mL reduction after 60 min, whereas KAMV, JEV, and FCV titers decreased significantly to below detection limits by 30, 10, and 1 min, respectively (Figure 2). Furthermore, even at 94°C, infectious SFTSV somehow persisted for 1 min with just 1.94 log10 ffu/mL reduction, whereas KAMV, JEV, and FCV were rapidly inactivated to below detection limits within 1 min (Figure 2). These results suggest that SFTSV potentially possesses a resistance against heat inactivation.

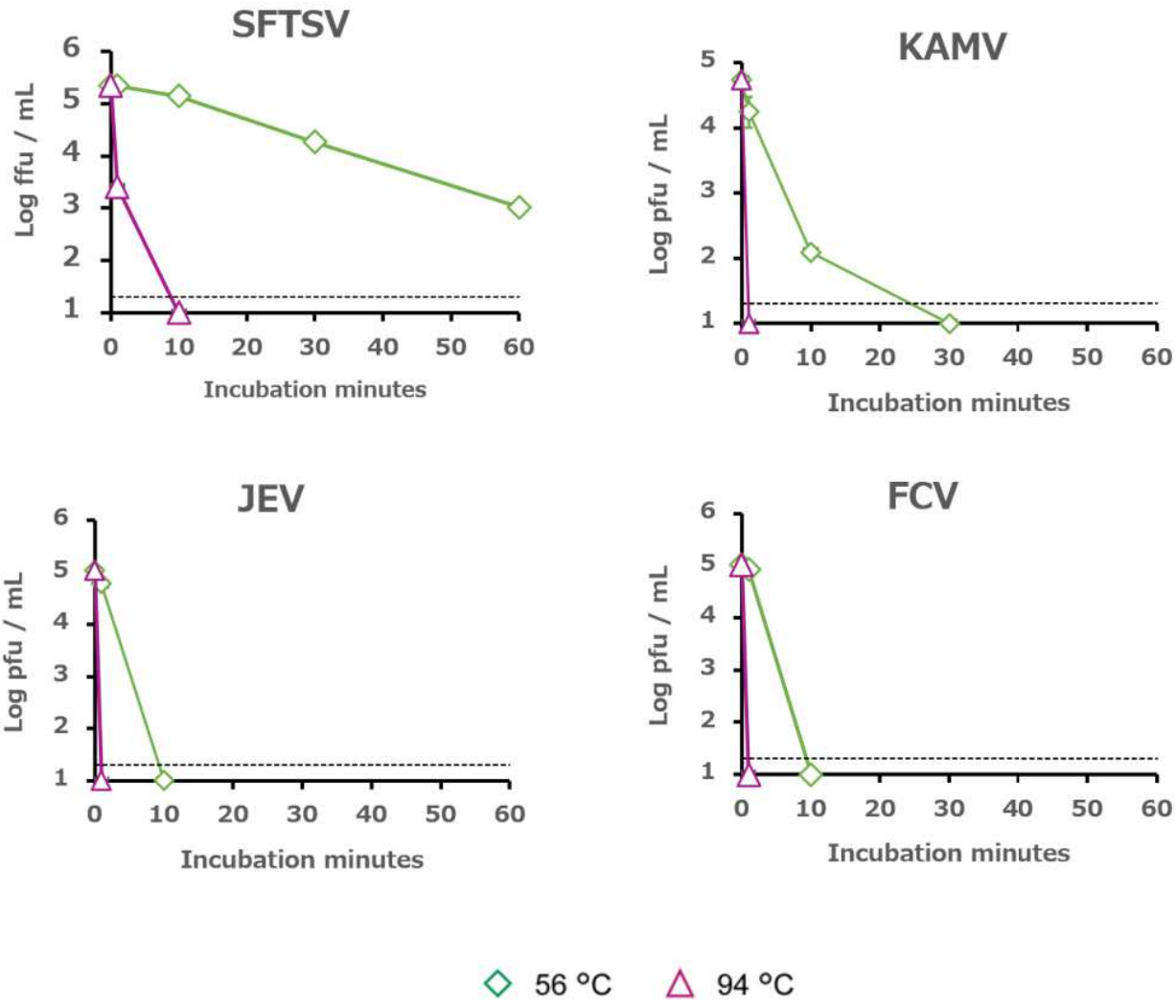


Fig. 2.2 Viral infectious titers of Severe fever with thrombocytopenia syndrome virus (SFTSV), Kabuto Mountain virus (KMV), Japanese Encephalitis virus (JEV), and Feline Calicivirus (FCV) after incubation at 56°C and 94°C. Approximately 1.25×10^5 ffu/mL of each virus in 0.25 mL of 2% FCS MEM were incubated at 56°C and 94°C, and samples were collected after 1, 10, 30, and 60 min. Viral titers were measured as ffu/mL (SFTSV) or pfu/mL (KAMV, JEV, and FCV). Control viral titers (day 0) were $10^{5.34}$ ffu/mL (SFTSV), $10^{4.74}$ pfu/mL (KAMV), $10^{5.03}$ pfu/mL (JEV), and $10^{5.03}$ pfu/mL (FCV). Each data point was obtained from three independent experiments at the specified time points. Error bars indicate standard errors. The dotted line indicates the detection limit of SFTSV ($10^{1.3}$ ffu/mL).

2.4.3 Infectious Stability of SFTSV-Infected Mice Blood at 4°C, 23°C, 37°C, 56°C and 94°C

To confirm the infectious stability of SFTSV in clinical samples and assess the potential risk of infection in clinical practice, blood samples were prepared and evaluated for stability at different temperatures. A pooled blood sample from SFTSV-infected A129 mice was prepared to contain a high viral titer of $10^{6.33}$ ffu/mL. Those aliquots were incubated at 4°C, 23°C, 37°C, 56°C, and 94°C, and infectious titers were measured daily (Figure 3). Infectious titers did not decrease over 7 days at 4°C and 23°C and showed just a 1.72 log10 ffu/mL reduction at 37°C after 7 days (Figure 3A). At 56°C, infectious titers did not significantly decrease after 10 min, and the reductions were limited even after 60 min with a 1.98 log10 ffu/mL reduction (Figure 3B). At 94°C, 1 min incubation showed only a 1.14 log10 ffu/mL reduction (Figure 3B). These observations suggest that SFTSV-contaminated clinical samples possess infectious stability at lower to higher temperatures, and heat inactivation requires sufficient incubation time for SFTSV-contaminated clinical samples.

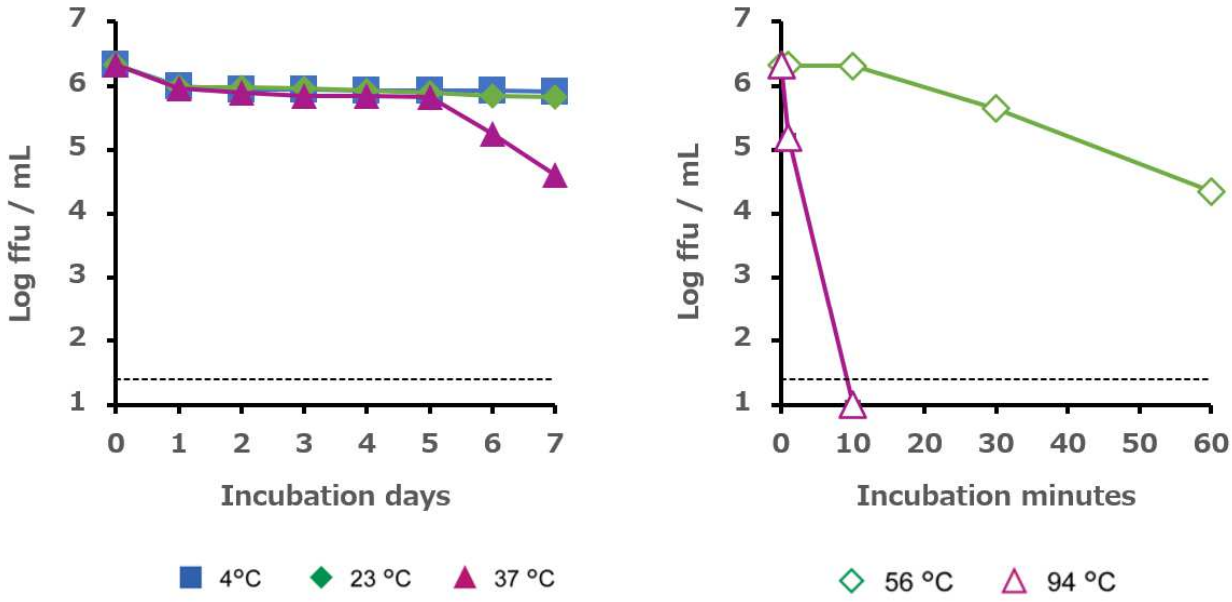


Fig. 2.3. Log-reduction of Severe fever with thrombocytopenia syndrome virus (SFTSV) infectivity in blood across varying temperatures. The virus titers of the recovered viruses were measured as ffu/mL. Control viral titers (day 0) was $10^{6.33}$ ffu/mL. Each data point was obtained from three independent experiments at the specified time points. Error bars indicate standard errors. The dotted line indicates the detection limit of SFTSV ($10^{1.3}$ ffu/mL).

2.4.4 Virucidal Efficacy of Ethanol and Sodium Hypochlorite on SFTSV Infectivity

High-temperature stability and resistance to heat inactivation of SFTSV raised an infectious risk at clinical sites where SFTSV-infected animals are treated. Thus, to confirm the appropriate methods for reducing the risk, we examined the efficacy of common disinfectants, ethanol, and sodium hypochlorite against SFTSV. Exposure to 70% ethanol and 100 ppm sodium hypochlorite resulted in complete loss of viral infectivity within 1 min (Figure 4). Thus, it is suggested that these detergents show sufficient virucidal effects against SFTSV and are useful for reducing the risk of SFTSV infection from clinical samples.

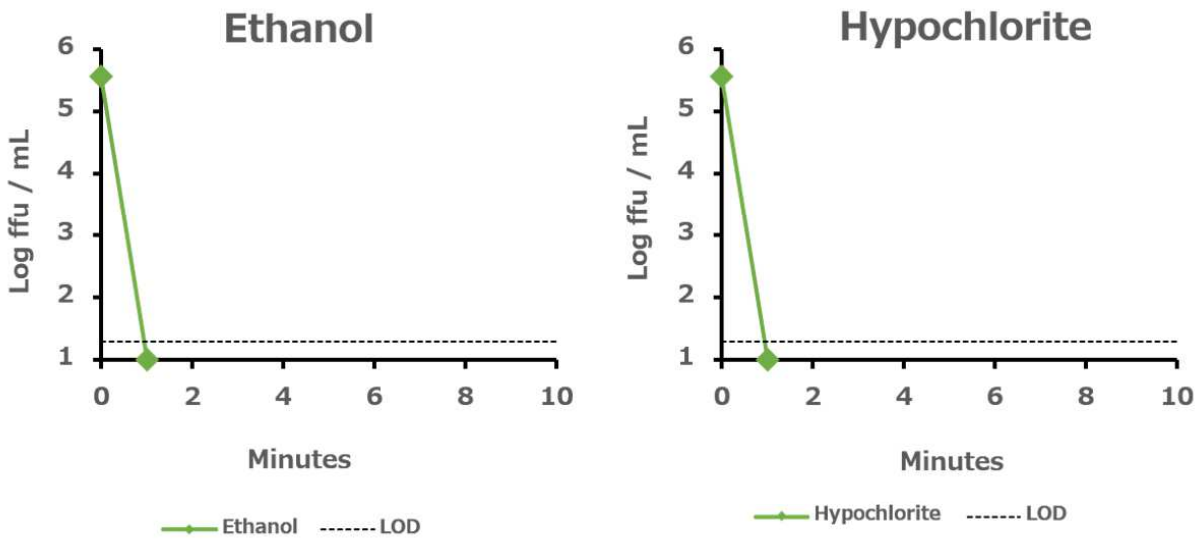


Fig. 2.4 Viral infectious titers of Severe fever with thrombocytopenia syndrome virus (SFTSV) after treatment with 70% ethanol and sodium hypochlorite solutions. Control viral titers (day 0) was $10^{5.56}$ ffu/mL. Each data point was obtained from three independent experiments at the specified time points. Error bars indicate standard errors. The dotted line indicates the detection limit of SFTSV ($10^{1.3}$ ffu/mL).

2.4.5 Inactivation Efficacy of UV Irradiation on SFTSV Infectivity

We also evaluated the inactivation efficacy of UV against SFTSV using 254nm UV-CCL, 265nm DUV-LED, and 275nm DUV-LED irradiations. Compared to the non-irradiated control (5.22 log10 ffu/mL), the infectious titers were significantly reduced by 254 nm (20 sec of radiation: 2.84 log10 ffu/mL), 265 nm (28 sec of radiation: 1.79 log10 ffu/mL), and 275 nm (60 sec of radiation: 1.56 log10 ffu/mL). Based on these data, UV doses (mJ/cm2) were calculated for the inactivation of SFTSV (Figure 5). The UV doses required to achieve a 2-log reduction in virus titers were 2.99, 3.57, and 5.44 mJ/cm^2 following 254 nm UV-CCL, 265 nm DUV-LED, and 275 nm DUV-LED irradiation, respectively (Figure 5). These data indicate that UV irradiation is effective at inactivating SFTSV, with shorter wavelengths being more effective.

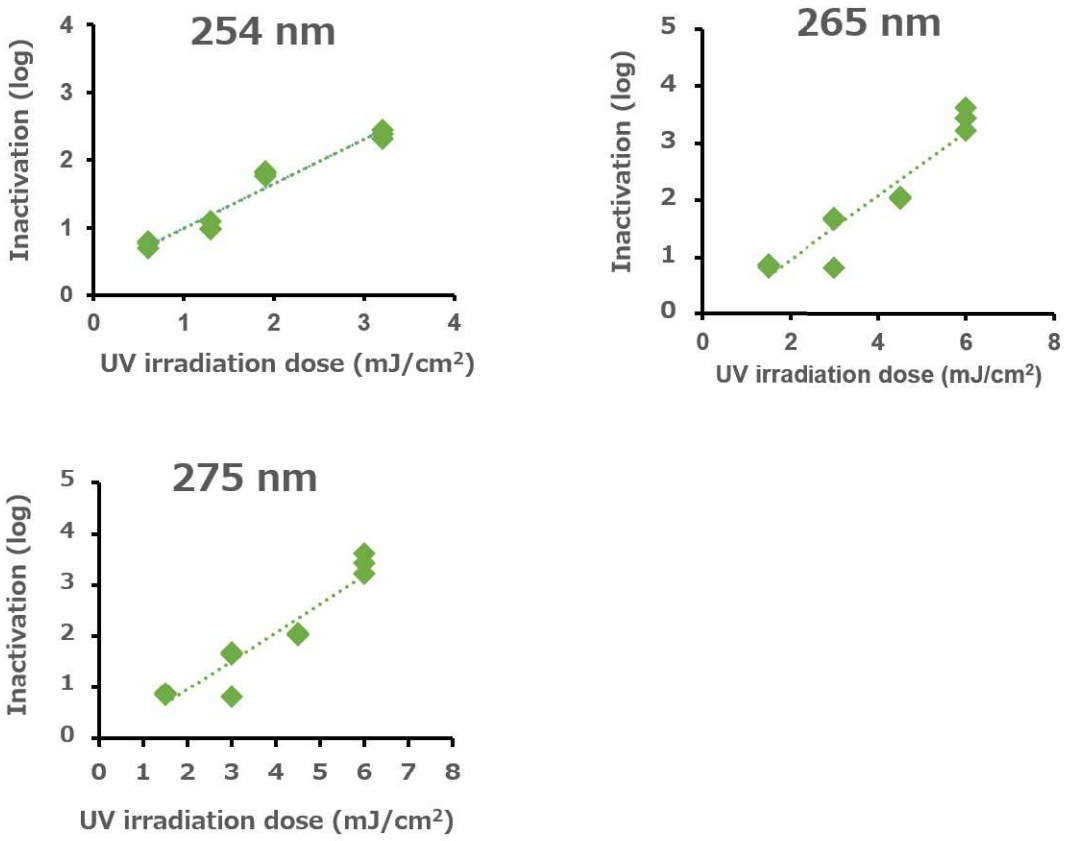


Fig. 2.5 Inactivation rates of Severe fever with thrombocytopenia syndrome virus (SFTSV) by UV light. The X-axis indicates the UV radiation dose, and the Y-axis indicates the inactivation rate of the log phase. Each data point was obtained from three independent experiments, and each line indicates the approximation line calculated from the results of each wavelength.

2.5 Discussion

In this study, we showed a temperature-dependent resistance of SFTSV. The infectivity of SFTSV was sustained at 4°C to 37°C for several days compared to the enveloped JEV, KAMV, and the non-enveloped FCV, suggesting that SFTSV-contaminated samples may retain the infectivity at room temperature conditions throughout the seasons. In addition, SFTSV has a comparative resistance against heat inactivation conditions at 56°C and 94°C. In particular, the inactivation effect of SFTSV was limited under the general complement inactivation condition for serum at 56°C for 30 min. On the other hand, SFTSV was easily inactivated by ethanol, hypochlorite, and UV irradiation, indicating that an inactivation procedure by appropriate treatment is important to reduce the risk of SFTSV infection from the contaminated samples at clinical sites and laboratories.

The increased stability of SFTSV at higher temperatures, especially 56°C and 94°C, highlights its remarkable heat tolerance. This thermotolerance may be associated with multiple structural features of SFTSV. Accumulating evidence suggests that certain members of the bunyaviruses exhibit structural features that enhance virion stability (Walter & Barr, 2011; Halldorsson et al., 2018; Uckeley et al., 2024). Cryo-electron microscopy studies of SFTSV have demonstrated that the Gn and Gc glycoproteins form an organized, lattice-like surface architecture that contributes to envelope rigidity and particle integrity (Lokupathirage et al., 2021; Du et al., 2023). Such ordered glycoprotein assemblies may be responsible for the reduction in conformational disruption under transient thermal stress (Liu Q et al., 2014; Du et al., 2023). Previous studies have indicated that some filoviruses and bunyaviruses have significant heat resistance (Piercy et al., 2010; Walter & Barr, 2011; Beniac et al., 2012). This resistance can be mechanistically linked to the virus's cholesterol-rich membranes and the highly ordered structures of its nucleocapsid glycoproteins, which provide thermal protection (Piercy et al., 2010; Walter & Barr, 2011; Beniac et al., 2012). During budding, bunyaviruses acquire host-derived lipids, including cholesterol, and cholesterol-embedded membranes have been shown to increase membrane packing density and provide resistance to thermal perturbation (Frieberg et al., 2008; Uckeley et al., 2024). In addition, the ribonucleoprotein, which forms stable complexes of SFTSV, is also tightly encapsulated by nucleoprotein, forming stable helical structures that may protect genomic RNA from heat-induced degradation (Jiao et al., 2013; Zhou et al., 2013). Importantly, the observation that SFTSV retains infectivity at near-boiling temperature (94°C) is a novel finding that greatly advances our understanding of its thermotolerance and suggests potential adaptations that could facilitate viral survival across different environments. Further structural and mechanistic analyses will be necessary to identify the specific molecular factors responsible for the thermal resistance of SFTSV.

Another important finding in our study is the sustained infectivity of SFTSV at 23°C and 37°C. Although previous studies showed that SFTSV infection risk increases at temperatures below 17°C (Sun et al., 2021), our results demonstrate that SFTSV remains highly infectious at both 23°C and 37°C. This suggests that SFTSV-contaminated bodily fluids could pose a significant transmission risk within these temperature ranges, which is a potential threat to vulnerable populations. Our findings highlight the importance of monitoring environmental conditions and their effects on SFTSV infectivity, which could help shape public health strategies to reduce transmission risk.

Exposure to low temperatures, such as 4°C, significantly enhances viral stability by slowing physicochemical processes that lead to structural degradation and loss of infectivity (Kampf et al., 2020). This stabilization reduces molecular motion and preserves ribonucleoprotein complexes. (Rabenau et al., 2005; Kampf et al., 2020). The enhanced stability of SFTSV at 4°C aligns with these principles and may also be attributed to the orderly arrangement of its lipid bilayer envelope, which reduces fluidity and makes it less susceptible to disruption (Darnell et al., 2004; Kampf et al., 2020). The relatively high stability of SFTSV at 4°C may be advantageous for long-term storage and transportation to the institutes where a diagnosis of SFTS is conducted at the request of clinical hospitals.

Chemical disinfection assays demonstrated that SFTSV infectivity is effectively eliminated by 70% ethanol and sodium hypochlorite. Detergents and chlorine-based disinfectants disrupt viral lipid envelopes, resulting in loss of infectivity, and enveloped viruses are consistently susceptible to these agents (Rutala & Weber, 2008; Cutts et al., 2020). These results indicate that commonly used disinfectants are effective against SFTSV and support their continued use for surface and equipment decontamination in veterinary clinical and laboratory environments. However, the effectiveness of disinfectant may decrease in the presence of organic materials such as blood, serum proteins, or tissue debris, which can hinder chemical activity (Araújo et al., 2013; Campagna et al., 2016; Allingham et al., 2024). Thus, further detailed evaluation under conditions of organic material contamination will provide more useful information for reducing the risk of infection from SFTSV-contaminated samples in clinical practice.

UV-C irradiation resulted in wavelength-dependent inactivation of SFTSV. UV-C wavelengths (200-280nm) inactivate viruses primarily by damaging viral nucleic acids or proteins, thereby impairing replication (Song et al., 2010; Shimoda et al., 2021). These findings are consistent with previous work demonstrating a significant reduction in SFTSV infectivity with UV-LED irradiation at 280 ± 5 nm (Kaneko et al., 2022). However, the energy required for inactivation in the present study was lower. This difference underscores the importance of wavelength selection and system optimization

in the application of UV-LED technology for viral inactivation. Furthermore, UV irradiation is limited by line-of-sight exposure and surface irregularities, which cause shadowing, scattering, or absorption of UV light. These factors decrease the UV dose received by the organism and reduce the methodological efficiency (Christensen & Linden, 2003; Friedler et al., 2021; Palma et al., 2025). Therefore, proper pre-cleaning and appropriate UV system designs are important for achieving effective reductions in real-world settings.

From a veterinary microbiology perspective, the demonstrated stability of SFTSV across a range of temperatures has important implications for infection control. The virus's ability to retain infectivity during sample storage, transportation, and routine handling underscores the need for validated inactivation procedures when processing clinical specimens from animals in endemic regions. Although our current data do not show the specific mechanism of SFTSV stability, future research employing biophysical or structural analyses will be required to reveal the specific mechanisms.

2.6 Conclusion

This chapter showed that SFTSV retains infectivity across a broad temperature range, including extreme heat, demonstrating remarkable thermal stability. Structural features of the virion likely contribute to this resilience and may facilitate environmental persistence. Although 70% ethanol, sodium hypochlorite, and UV-C effectively inactivated the virus, reduced efficacy in the presence of organic material highlights the need for proper specimen handling and pre-cleaning procedures. These findings reinforce the transmission risk posed by contaminated materials and support further studies to define the molecular basis of SFTSV thermotolerance

Chapter 2: Comparison of Pathogenicity in IFN-I Interferon Receptor-Deficient A129 Mice and Characterization of Amino Acid Substitutions among Severe Fever with Thrombocytopenia Syndrome Virus Strains

3.1 Abstract

Severe fever with thrombocytopenia syndrome virus (SFTSV) is an emerging tick-borne zoonotic pathogen endemic to Asian countries, including Japan. We previously demonstrated that a pair of amino acid residues, Gly_{581} and Ser_{934} in the Gc of SFTSV, are key determinants of virulence in type I interferon receptor-deficient A129 mice. However, whether additional viral factors contribute to strain-dependent differences in pathogenicity remains unclear. In this study, we further observed the pathogenicity of fourteen SFTSV strains, including newly isolated strains from SFTS cat cases, in A129 mice. Fatality rates ranged from 20% to 100%. Notably, all strains, including those with low fatality, possessed the virulent Gly_{581} and Ser_{934}, suggesting that other substitutions influence the pathogenicity. Focusing on Sh-F149 and Yg-F197 with reduced virulence (40% fatality), we found unique amino acid substitutions. Sh-F149 possessed Ile_{745} in the Gc, and Yg-F197 exhibited Thr_{172} in the NSs, Gly_{20} and Arg_{113} in the Gn, and Arg_{307}, Val_{371}, Pro_{374}, and Asn_{1610} in the RdRp. No significant differences in viral growth kinetics were observed among strains in Vero E6 and TLT cells, and phylogenetic analysis showed that all strains belonged predominantly to genotype J1. These findings indicate that neither in vitro replication efficiency nor genotype alone accounts for virulence differences in A129 mice. Taken together, our results suggest that strain-specific amino acid substitutions contribute to SFTSV pathogenicity and provide a basis for future mechanistic studies.

3.2 Introduction

Severe fever with thrombocytopenia syndrome (SFTS) is an emerging zoonotic viral disease endemic to Asian countries, including China, South Korea, Vietnam, Taiwan, and Japan (Yu et al., 2011; Kim et al., 2013; Takahashi et al., 2014; Tran et al., 2019; Lin et al., 2020). In human cases, SFTS presents with symptoms such as fever, gastrointestinal issues, thrombocytopenia, leukopenia, and multi-organ failure with a fatality rate of up to 30% (Yu et al., 2011; Liu Q et al., 2014; Kim et al., 2018). In addition, a variety of domestic and wild animals are susceptible to SFTSV infection (Niu et al., 2013; Ding et al., 2014; Tabara et al., 2016), and cats are particularly susceptible and often develop severe or fatal illnesses (Matsuu et al., 2019). The causative agent, SFTSV, is transmitted by ticks (Gai et al., 2012; Fang et al., 2021), and human-to-human infection through blood or bodily fluids has also been reported (Yamanaka et al., 2020; Kirino et al., 2021; Tsuru et al., 2021). In addition, SFTSV infections from animals to humans have been reported (Kida et al., 2019; Tsuru et al., 2021; Li et al., 2024), highlighting their potential role as a source of zoonotic infections and emphasizing the need to better understand the pathogenic characteristics of SFTSV.

SFTSV is classified within the family *Phenuiviridae*, genus *Bandavirus*, and species *Bandavirus dabieense*. The virus consists of a segmented negative-strand RNA genome with small (S), medium (M), and large (L) segments. The S segment is ambisense, encoding two proteins: the antisense RNA encodes nucleoprotein (NP), while the sense RNA encodes non-structural proteins (NSs) (Yu et al., 2011; Kim et al., 2013; Brennan et al., 2015). The M segment encodes viral glycoproteins (GPs), which are processed into two viral envelope glycoproteins, Gn and Gc (Yu et al., 2011; Brennan et al., 2015; Lei et al., 2015). The L segment encodes the RNA-dependent RNA polymerase (RdRp), which functions as the viral replicase (Yu et al., 2011; Lei et al., 2015; Reguera et al., 2016).

Domestic cats have been recognized as potential sources of zoonotic transmission of SFTSV to humans, and several human infections have been linked to contact with infected companion animals (Matsuno et al., 2018; Matsuu et al., 2019). Therefore, the variation in pathogenicity observed among cat-derived strains may have implications for disease severity and transmission risk in both animals and humans. Understanding the molecular determinants that influence pathogenicity in cat-derived SFTSV strains may contribute to improved risk assessment and surveillance strategies within a One Health framework.

Previous studies have demonstrated that both viral and host factors contribute to the high pathogenicity of SFTSV (Yoshikawa et al., 2019; Wang et al., 2024; Xing et al., 2025). To investigate viral determinants of virulence *in vivo*, type I

interferon receptor knockout ($IFNAR^{-/-}$) mouse models, including A129 mice, have been widely used (Liu Y et al., 2014; Shimada et al., 2015; Tani et al., 2016). Previously, using comparative analyses between two SFTSV strains, Tk-F123 and Ng-F264, in $IFNAR^{-/-}$ A129 mice, we showed that a pair of amino acid residues at positions 581 and 934 in the Gc determine the pathogenicity of SFTSV in the mouse model (Wulandari et al., 2025). Using this model, we previously showed that a pair of amino acid residues at positions 581 and 934 in the Gc is a critical determinant of pathogenicity (Wulandari et al., 2025). Specifically, Gly_{581} and Ser_{934} in the Tk-F123 strain were associated with increased virulence, whereas Arg_{581} and Asp_{934} in the Ng-F264 strain were linked to attenuated pathogenicity (Wulandari et al., 2025).

However, this pair of residues alone is unlikely to fully account for the observed variability in virulence among SFTSV strains. Indeed, accumulating evidence suggests that additional viral genetic factors may modulate pathogenicity in a strain-dependent manner. In this study, we compared the pathogenicity of fourteen cat-derived SFTSV strains in A129 mice and performed comprehensive sequence analyses to find amino acid substitutions associated with reduced virulence. These results will provide new insights into the elucidation of SFTSV pathogenicity and virulence.

3.3.0 Materials and Methods

3.3.1 Viruses and Cells

Fourteen SFTSV strains, Tk-F123, Ng-F264, Ng-F95, Ng-F125, Sh-F149, Yg-F157, Yg-F180, Ng-F186, Yg-F197, Ng-F206, Fk-F258, Ng-F265, Yg-F267, and Yg-F274, were isolated from serum or plasma samples of cats diagnosed with SFTS at our laboratory between 2021 and 2022 (Table 1). Vero E6 cells and Tiger Liver Tumor (TLT) cells previously established in our laboratory (Anggita et al., 2025), were cultured in Dulbecco's Modified Eagle's Medium (DMEM; Thermo Fisher Scientific, Waltham, MA, USA), supplemented with 10% heat-inactivated fetal bovine serum (FBS; Serena Europe GmbH, Pessin, Germany), and 1% penicillin-streptomycin (100 U/mL penicillin and 100 µg/mL streptomycin; FUJIFILM, Wako Pure Chemical Corporation, Osaka, Japan), at 37°C in a 5% CO_2 incubator. SFTSV strains were initially isolated in Vero E6 cells cultured in DMEM containing 2% FBS. Culture supernatants were harvested at 5 days post-infection and passaged once in Vero E6 cells to generate working stocks, which were stored at -80°C until use. Experiments with infectious SFTSV were conducted in a biosafety level-3 (BSL-3) laboratory at Yamaguchi University in accordance with standard BSL-3 guidelines.

3.3.2 Focus Forming Assay (FFA)

Infectious viral titers were determined by FFA as previously described (Hayasaka et al., 2015). Briefly, confluent Vero E6 cells were inoculated with serial dilutions of virus-containing supernatants. After adsorption, cells were overlaid with DMEM containing 2% FBS and 1% methylcellulose and incubated (Wako Pure Chemical Industries, Ltd) for 3 days. Viral foci were detected using a mouse monoclonal antibody against SFTSV nucleoprotein (Yu et al., 2011), followed by peroxidase-conjugated anti-mouse IgG (American Qualex, San Clemente, CA, USA), and visualization with DAB substrate (FUJIFILM Wako Pure Chemical Corporation). Viral titers were expressed as focus-forming unit (ffu/mL).

3.3.3 SFTSV Infection in Mice

$IFNAR^{-/-}$ A129 mice were obtained from B&K Universal Limited and mated at Yamaguchi University. Six- to eight-week-old A129 mice (n = 5 per group, including both males and females) were subcutaneously inoculated with 10^4 FFU of

SFTSV diluted in 2% FBS DMEM. Mice were monitored daily for clinical signs and body weight. Humane endpoints were defined in accordance with guidelines criteria, and mice that reached the endpoint were euthanized by isoflurane overdose. Animal experiments were conducted in compliance with the Fundamental Guidelines for the Proper Conduct of Animal Experiments and Related Activities in Academic Research Institutions under the jurisdiction of the Ministry of Education, Culture, Sports, Science, and Technology, and were approved by the Animal Care and Use Committee of Yamaguchi University (approval number: 05-31-565).

3.3.4 Quantification of Viral RNA

Liver, kidney, and brain tissues were collected from mice infected with SFTSV strains, Tk-F123, Ng-F125, Ng-F265, Yg-F197, and Ng-F264, at 3 days post-infection (dpi). Tissues were homogenized in phosphate-buffered saline using a TOMY Micro Smash MS-100 homogenizer (TOMY Digital Biology Co., Ltd., Tokyo, Japan). Total RNA was extracted using ISOGEN II (Nippon Gene Co., Ltd) according to the manufacturer's instructions. Viral RNA copy numbers were determined by quantitative real-time RT-PCR (qRT-PCR) using the RdRp-specific primers as previously described (Hayasaka et al., 2015; Ando et al., 2021). Reactions were performed using a One-Step PrimeScript RT-PCR Kit (Takara Bio Inc., Shiga, Japan), on a CFX96 Touch Real-Time PCR Detection System (Bio-Rad, Hercules, CA, USA).

3.3.5 Viral Genome Sequencing and Phylogenetic Analysis

The entire viral genome of the SFTSV strains were sequenced as previously described (Yu et al., 2011). Briefly, viral RNA was extracted from stock viruses using Isogen-LS (Nippon Gene Co., Ltd). The S, M, and L segments were amplified by one-step RT-PCR using segment-specific primers (QIAGEN, Foster City, CA, USA). PCR products were purified using the MiniElute Gel extraction kit (QIAGEN, Hilden, Germany) and sequenced by the Sanger method (Eurofins Genomics, Tokyo, Japan). The GenBank accession numbers are listed in Table 1.

Phylogenetic trees for the S, M, and L segments were constructed using the maximum likelihood method implemented in IQ-TREE via Galaxy Europe software (Kalyaanamoorthy et al., 2017; Minh et al., 2020). The best-fit substitution models were selected as follows: GTR+F+I+R3 for the L segment, GTR+F+R3 for the M segment, and TvM+F+I+G4 for the S segment. Branch support was assessed using 1,000 bootstrap replicates. Trees were rooted using the midpoint method for intraspecies comparisons.

3.3.6 Virus Growth Kinetics

Confluent Vero E6 and TLT cells were inoculated with SFTSV strains at a multiplicity of infection (MOI) of 0.01. Supernatants of infected cells were harvested at 0, 1, 3, and 5 dpi and stored at -80°C. The samples were titrated using FFA. The experiment was performed in triplicate, with two independent experiments.

3.3.7 Statistical Analysis

One-way ANOVA with Tukey's test was performed to compare RNA levels in mouse tissues using GraphPad Prism. *(∗P ≤ 0.05)*

3.4.0 RESULTS

3.4.1 The Pathogenicity of SFTSV Strains in Infected Cats and A129 Mice

Twelve SFTSV strains, Ng-F95, Ng-F125, Sh-F149, Yg-F157, Yg-F180, Ng-F186, Yg-F197, Ng-F206, Fk-F258, Ng-F265, Yg-F267, and Yg-F274, were isolated from SFTS cat cases involving 7 fatal, 4 recovered, and 1 unknown outcomes in Japan (Table 1). These strains, and Tk-F123 and Ng-F264, were subcutaneously infected in A129 mice, and disease progression was compared to monitor fatality. Ng-F95, Yg-F180, Ng-F186, Ng-F206, Fk-F258, Yg-F267, Yg-F274 and Tk-F123 exhibited 100% fatality (Figure 3.1A and Table 3.1). Fatality of Ng-F125 and Yg-F157 were 80%, and that of Ng-F265 was 60%. Sh-F149 and Yg-F197 showed a low fatality of 40%. Ng-F264 showed no mortality in our previous study; it exhibited a 20% lower mortality in the present study (Figure 3.1A and Table 3.1).

Table 3.1 Cat-derived SFTSV strains used in this study

Strains	Year	Place	Fate	GenBank accession numbers		
				S	M	L
Tk-F123*	2021	Tokushima	Fatal	PZ322986	PZ323000	PZ323014
Ng-F264*	2022	Nagasaki	Unknown	PZ322995	PZ323009	PZ323023
Ng-F95	2021	Nagasaki	Fatal	PZ322985	PZ322999	PZ323013
Ng-F125	2021	Nagasaki	Fata	PZ322987	PZ323001	PZ323015
Sh-F149	2021	Shimane	Fatal	PZ322988	PZ323002	PZ323016
Yg-F157	2021	Yamaguchi	Recovered	PZ322989	PZ323003	PZ323017
Yg-F180	2021	Yamaguchi	Fatal	PZ322990	PZ323004	PZ323018
Ng-F186	2021	Nagasaki	Fatal	PZ322991	PZ323005	PZ323019
Yg-F197	2021	Yamaguchi	Recovered	PZ322992	PZ323006	PZ323020
Ng-F206	2021	Nagasaki	Fatal	PZ322993	PZ323007	PZ323021
Fk-F258	2022	Fukuoka	Unknown	PZ322994	PZ323008	PZ323022
Ng-F265	2022	Nagasaki	Recovered	PZ322996	PZ323010	PZ323024
Yg-F267	2022	Yamaguchi	Recovered	PZ322997	PZ323011	PZ323025
Yg-F274	2022	Yamaguchi	Fatal	PZ322998	PZ323011	PZ323026

*Previously reported strains in Wulandari et al., 2025.

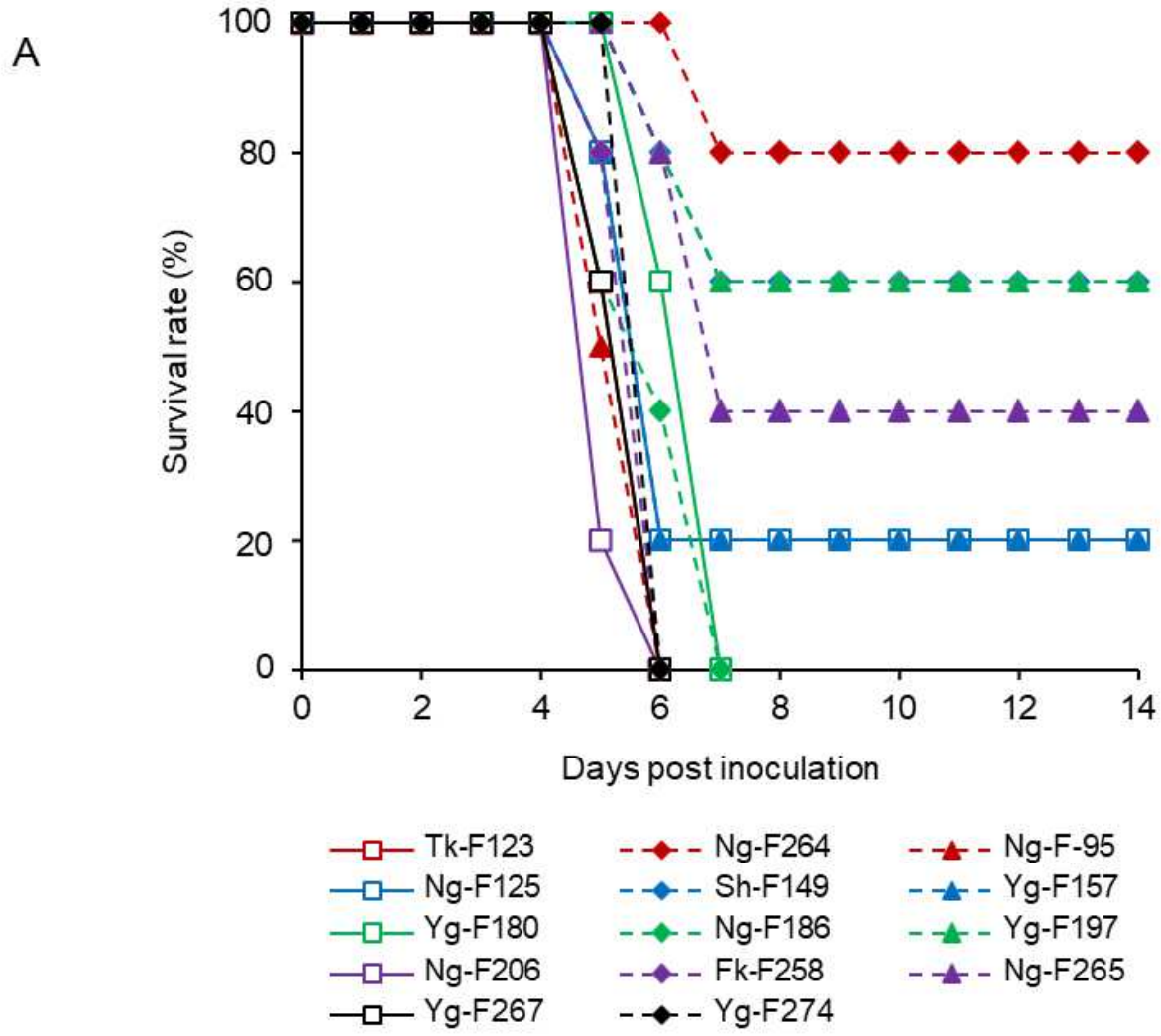


Fig. 3.1A Pathogenicity of cat-derived severe fever with thrombocytopenia syndrome virus strains in type-I interferon receptor-deficient A129 mice. Survival curves of mice subcutaneously infected with 10^4 ffu of Tk-F123, Ng-F264, Ng-F95, Ng-F125, Sh-F149, Yg-F157, Yg-F180, Ng-F186, Yg-F197, Ng-F206, Fk-F258, Ng-F265, Yg-F267, and Yg-F274 (n=5).

3.4.2 Viral Loads in Organs of SFTSV-infected Mice with Fatality Rates of 20-100%

Viral RNA levels in the liver and kidney, as representative peripheral organs, and the brain, as the central nervous system, were examined in mice infected with Ng-F264, Yg-F197, Ng-F265, Ng-F125, and Tk-F123 strains that showed 20%, 40%, 60%, 80%, and 100% fatality, respectively. Higher viral RNA levels were observed in strains associated with a

higher mortality (Figure 3.1B), although no statistically significant differences were detected among groups by one-way ANOVA.

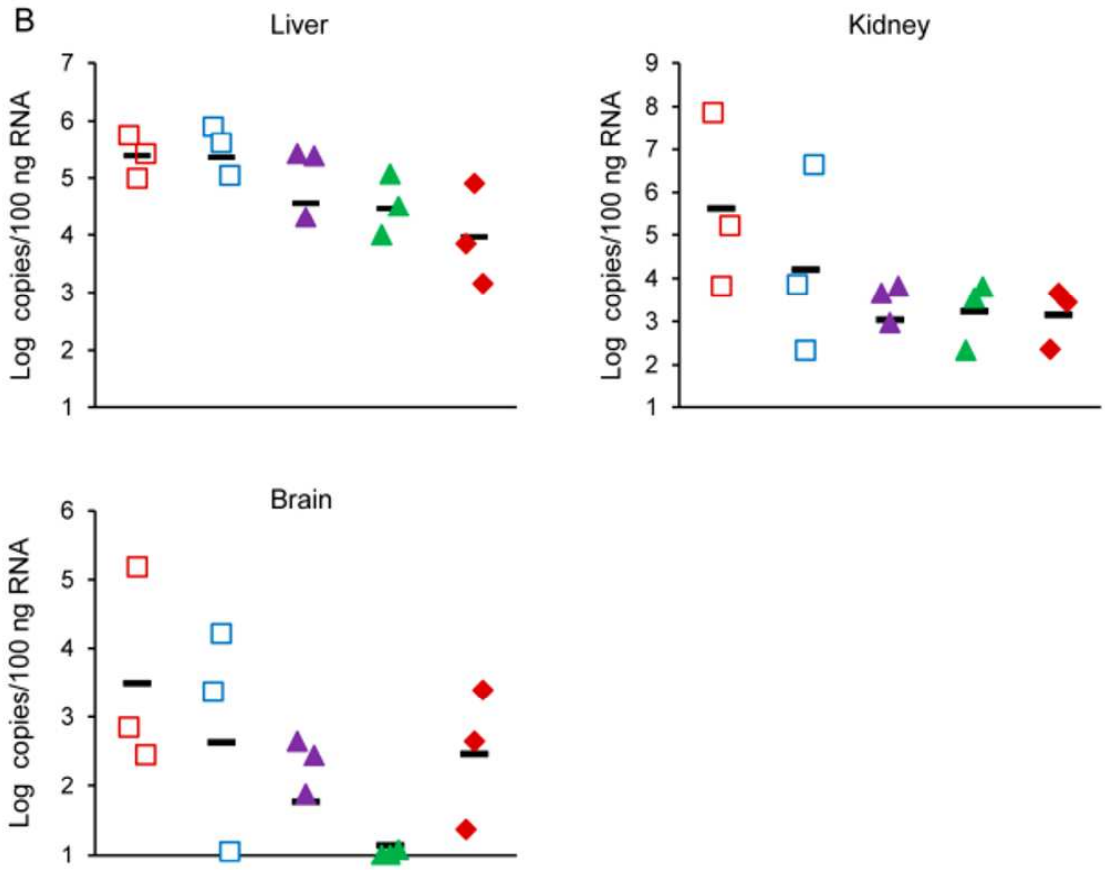


Fig. 3.1B Viral RNA copy numbers in tissues from mice infected with SFTSV strains Tk-F123, Ng-F125, Ng-F265, Yg-F197, and Ng-F264 (N=3). A one-way ANOVA with Tukey's multiple-comparison test was performed, but no significant differences were observed *(∗$P \leq 0.05$)*.

3.4.3 Amino Acid Substitutions of the Other SFTSV Strains Relative to TK-F123

Thus, we compared the amino acid sequences of the 12 SFTSV strains. In particular, Sh-F149 and Yg-F197, which exhibited 40% mortality, were analyzed in detail.

In the S segment, there were nucleotide variations at 53 nucleotide positions (data not shown), and three amino acid variations were found in the NSs (Table 3.2). Among these, Thr_{172} was uniquely present in Yg-F197. Asp_{238} was observed in both Sh-F149 and Yg-F197, but this amino acid was also observed in several highly pathogenic strains.

Table 3.2 Amino acid substitutions among Severe fever with thrombocytopenia syndrome virus (SFTSV) strains relative to the SFTSV Tk-F123 strain

		Strain	Tk-F123	Ng-F95	Yg-F180	Ng-F186	Ng-F206	Fk-F258	Yg-F267	Yg-F274	Ng-F157	Ng-F125	Ng-F265	Sh-F149	Yg-F197	Ng-F264
		Fatality	100	100	100	100	100	100	100	100	80	80	60	40	40	20
Segment	Gene	Position														
S	NSs	172	Ile	-	-	-	-	-	-	-	-	-	-	-	Thr*	-
-		236	Asp	-	-	-	-	-	Glu	-	-	-	Glu	-	-	-
		238	Glu	-	-	-	-	Asp	Asp	-	Asp	-	Asp	Asp	Asp	-
M	Gn	16	Gln	Arg	-	-	-	-	-	-	-	-	-	-	Arg	-
		20	Asp	-	-	-	-	-	-	-	-	-	-	-	Gly*	-
		93	Ser	-	-	-	-	Asn	-	-	Asn	-	-	Asn	-	-
		113	Lys	-	-	-	-	-	-	-	-	-	-	-	Arg*	-
		234	His	-	Tyr	-	-	-	-	-	-	-	-	-	-	-
		298	Ala	-	-	-	-	Thr	-	-	Thr	-	-	Thr	-	-
		339	Val	-	-	-	-	-	-	-	Met	-	-	-	-	-
		341	Ser	Pro	-	-	-	Pro	-	-	Pro	-	Pro	Pro	Pro	-
		385	Thr	-	-	-	-	-	-	-	-	-	-	-	-	Ala
		459	Val	Ala	-	-	-	-	-	-	-	-	-	-	Ala	-
		461	Leu	-	-	-	-	-	-	Val	-	-	-	-	-	-
		470	Leu	-	-	-	-	-	-	-	Val	-	-	-	-	-
	Gc	524	Asn	Tyr	-	-	-	-	-	-	-	-	-	-	Tyr	-
		530	Asp	-	-	-	-	-	-	Asn	Asp	-	-	-	-	-
		553	Thr	-	-	-	-	Ala	-	-	Ala	-	-	Ala	-	-
		581	Gly	-	-	-	-	-	-	-	-	-	-	-	-	Arg
		662	Ser	-	-	Pro	Pro	-	-	Pro	-	-	-	-	-	-
		745	Thr	-	-	-	-	-	-	-	-	-	-	Ile*	-	-
		926	Arg	Lys	-	-	-	Lys	-	-	Lys	-	-	Lys	Lys	-
		934	Ser	-	-	-	-	-	-	-	-	-	-	-	-	Asn
		960	Thr	-	-	-	-	Ala	-	Ala	-	-	-	-	-	-
L	RdRp	140	Ala	Thr	-	-	-	Thr	Thr	-	Thr	-	-	Thr	Thr	-
		240	Lys	-	-	-	-	-	-	-	-	Arg	-	-	-	-
		243	Gly	-	-	-	-	-	Glu	-	-	-	-	-	-	-
		285	His	-	-	-	-	-	-	Gln	-	-	-	-	-	-
		307	Lys	-	-	-	-	-	-	-	-	-	-	-	Arg*	Lys
		310	Asp	Glu	-	-	-	-	-	-	-	-	-	-	Glu	-
		314	Ser	-	-	-	-	-	-	-	-	Gly	-	-	-	-
		352	Phe	-	-	-	-	-	-	-	-	Tyr	-	-	-	-
		359	Gly	-	-	-	-	-	-	-	-	-	-	-	-	-
		371	Asp	-	-	-	-	-	-	-	-	-	-	-	Val*	-
		374	Leu	Ser	-	-	-	-	-	-	-	-	-	-	Pro*	-
		381	Ile	-	-	-	-	-	-	-	-	Val	-	-	-	-
		393	Ser	-	-	-	-	-	-	-	-	Phe	-		-	-

418	Ser	Asn	-	-	-	-	-	-	-	-	-	-	Asn	-
538	Ala	-	-	-	Thr	-	-	-	-	-	-	-	-	-
573	Ala	-	-	-	-	-	-	-	-	-	Val	-	-	-
818	Ala	-	-	-	-	-	-	-	-	-	Thr	-	-	-
884	Arg	Lys	-	-	-	Lys	Lys	-	Lys	Lys	-	Lys	Lys	-
1116	Asn	-	-	-	-	-	Ser	-	-	Ser	-	-	-	-
1353	Asn	Ser	-	-	-	-	-	-	-	-	-	-	Ser	
1363	Glu	Gly	-	-	-	-	-	-	-	-	-	-	-	-
1610	Ser	-	-	-	-	-	-	-	-	-	-	-	Asn*	-
1651	Ile	-	-	-	-	-	Met	-	-	-	-	-	-	-
1717	Ile	-	-	-	-	-	-	-	-	Val	-	-	-	-
1906	Arg	Lys	-	-	-	Lys	Lys	-	Lys	Lys	-	Lys	Lys	-
1943	Lys	-	-	-	-	-	-	-	-	Arg	-	-	-	-

*Unique amino acids in Sh-F149 and Yg-F197

In the M segment, there were nucleotide variations at 97 nucleotide positions (data not shown), and amino acid varieties were found at a total of 21 positions in the Gn and Gc (Table 3.2). It is noteworthy that all strains except Ng-F264, including Sh-F149 and Yg-F197, possessed the virulent pair of Gly_{581} and Ser_{934}. Sh-F149 amino acid sequences were closest to those of Fk-F258 that exhibited 100% fatality in A129 mice, and Sh-F149 exhibited a unique substitution, Ile_{745} in the Gc, compared with Thr_{745} of Fk-F258. Also, the amino acid sequences of Yg-F197 were closest to those of Ng-F95, which showed 100% fatality in A129 mice, and Yg-F197 showed unique substitutions Gly_{20} and Arg_{113} in the Gn compared with Asp_{20} and Lys_{113} of Ng-F95.

In the L segment, there were nucleotide varieties at 194 nucleotide positions (data not shown), and 13 amino acid variations were in the RdRp (Table 3.2). There were no amino acid differences between Sh-F149 and Fk-F258. On the other hand, Yg-F197 possessed four unique substitutions: Arg307, Val_{371}, Pro_{374}, and Asn_{1610} compared with Lys_{307}, Asp_{371}, Ser_{374}, and Ser_{1610} in Ng-F95 in the RdRp.

From these results, it was suggested that the unique amino acid of Ile_{745} in the Gc contributes to the attenuated pathogenicity of Sh-F149. Furthermore, Thr_{172} in the NSs, Gly_{20} and Arg_{113} in the Gn, and Arg_{307}, Val_{371}, Pro_{374}, and Asn_{1610} in the RdRp may be responsible for the attenuated pathogenicity of Yg-F197. Therefore, these amino acids are considered key factors that may be contributing to the attenuated pathogenicity of SFTSV in the A129 mouse model.

3.4.4 Growth Kinetics in VeroE6 and TLT Cell Lines

Our previous study indicated that there were no significant differences in virus growth properties *in vitro* (in cell cultures) among SFTSV strains exhibiting different fatality rates in A129 mice (Ando et al., 2021). Thus, to assess whether *in vitro* replication correlates with pathogenicity, the growth kinetics of five representative strains, Tk-F123, Ng-F125, Ng-F265, Yg-F197, and Ng-F264, were evaluated in highly susceptible SFTSV cell lines of Vero E6 and TLT (Anggita et al., 2025). Similar to our previous results, no significant differences in viral titers were observed among the strains at any time point in either cell line (Figure 3.2). Cytopathic effects in TLT cells and the absence of cytopathic effects in Vero E6 cells were comparable across all strains. (data not shown).

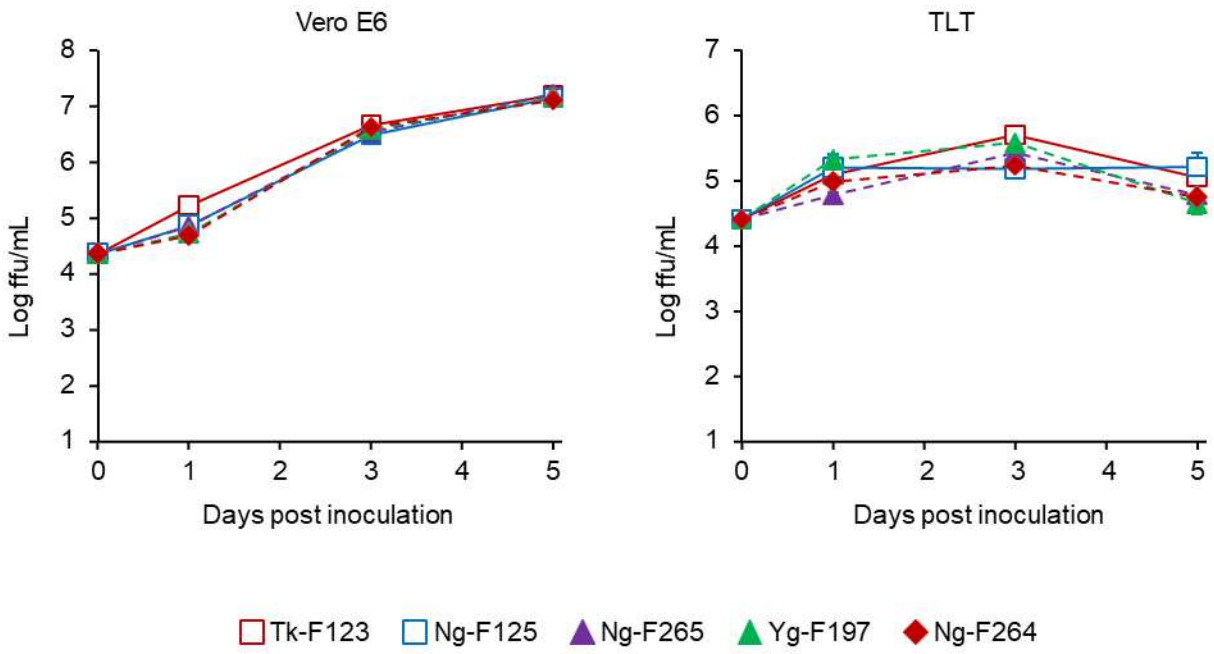


Fig. 3.2 Growth kinetics of severe fever with thrombocytopenia syndrome virus (SFTSV) strains. Cells were infected with SFTSV at a multiplicity of infection (MOI) of 0.01, and the supernatants were collected at 0, 1, 3, and 5 dpi. Starting viral loads were 2.34 x 10^4 and 2.59 x 10^4 ffu in Vero E6 and Tiger Liver Tumor (TLT) cell lines, respectively. Each experiment was performed in triplicate, with 2 independent experiments. Error bars indicate standard deviations.

3.4.5 Phylogenetic Analysis of the SFTSV Strains used In This study

We also examined whether pathogenicity in A129 mice correlated with the genotype of SFTSV strains. Phylogenetic analyses were performed using full-length sequences of the S, M, and L segments strains together with representative SFTSV strains from GenBank. All strains except for Ng-F125 were classified into genotype J1 based on all three genome segments (Figure 3.3A, 3.3B, and 3.3C). Ng-F125 was classified as genotype J1 based on S and M segments (Figure 3a and 3b) but as genotype J3 based on the L segment (Figure 3.3C), suggesting that Ng-F125 was a reassortant virus between J1 and J3 genotypes. It is noteworthy that no clear association was observed between phylogenetic classification and mortality rates among the SFTSV strains analyzed in this study.

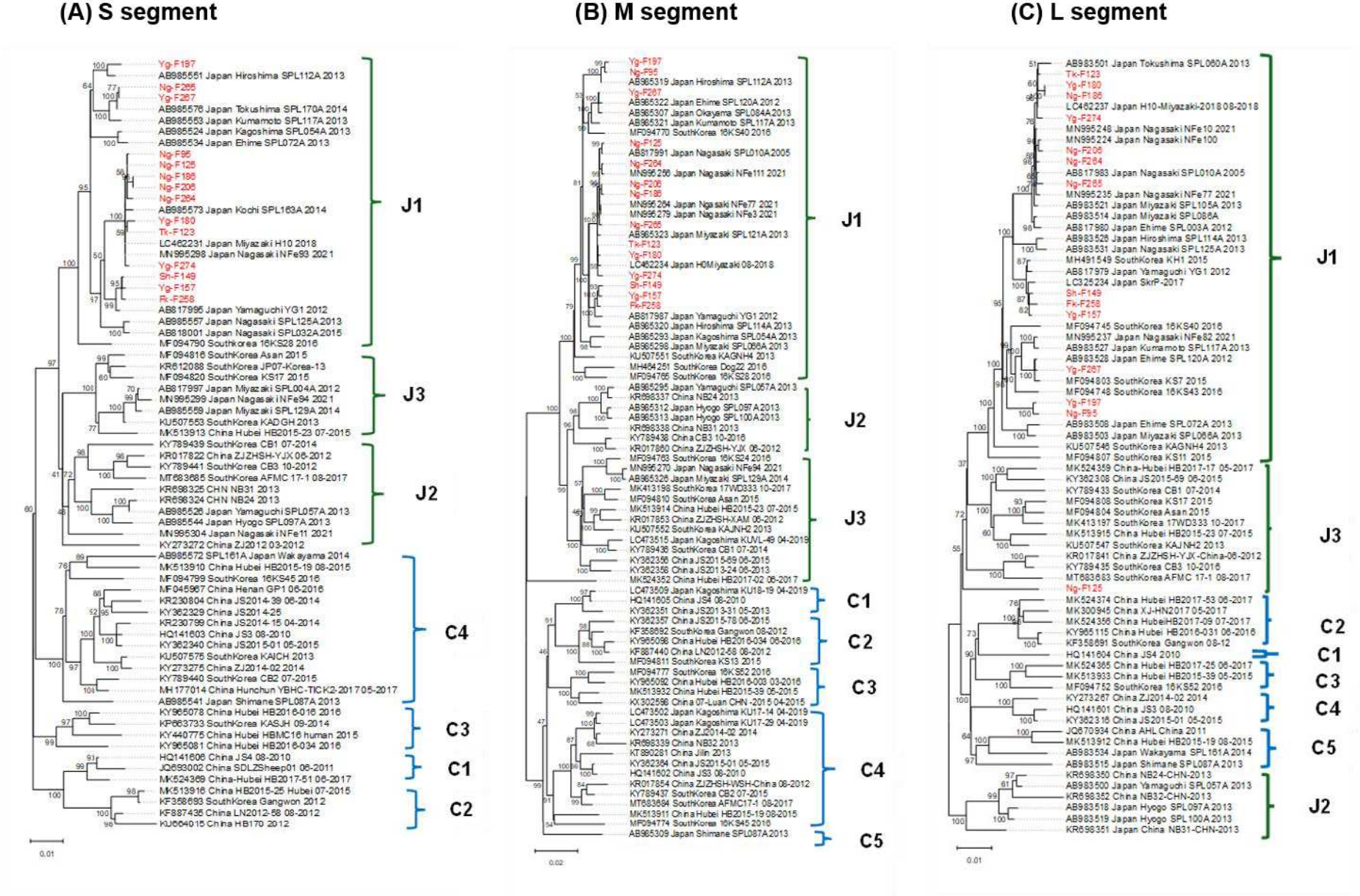

(A) S segment
(B) M segment
(C) L segment
J1
J3
J2
C4
C3
C1
C2
C5
0.01
0.02
0.01

Fig. 3.3 Phylogenetic trees based on the full-length nucleotide sequences of the severe fever with thrombocytopenia syndrome virus (SFTSV) strains for (A) S segment, (B) M segment, and (C) L segment. The SFTSV strains shown in red were analyzed in this study. Maximum-likelihood phylogenetic trees were reconstructed using IQ-TREE with the best-fit substitution model. Branch support values were estimated with 1,000 bootstrap replicates and are shown at the nodes. The tree was rooted using the midpoint method for intraspecies comparison.

3.5.0 Discussion

In this study, we observed amino acid residues of cat-derived SFTSV strains that may be potentially associated with fatality in A129 mice. We previously found that the pair of amino acid residues of Gly_{581} and Ser_{934} in the Gc is a determinant of the fatality in A129 mice (Wulandari et al., 2025). Interestingly, all SFTSV strains used in this study carried the fatal Gly_{581} and Ser_{934}; however, several strains exhibited lower fatality, suggesting that other viral amino acids may contribute to reduced pathogenicity. In particular, Sh-F149 and Yg-F197 exhibited comparatively low fatality rates of 40%, suggesting that the unique viral amino acids observed, Ile_{745} in Gc of Sh-F149 and Thr_{172} in NSs, Gly_{20}, and Arg_{113} in Gn, and Arg_{307}, Val_{371}, Pro_{374}, and Asn_{1610} in RdRp of Yg-F197, may likely contribute to attenuation of SFTSV pathogenicity. Of note, comparisons between the genetically closest pairs of Sh-F149 (40% fatality) and Fk-F258 (100% fatality), or Yg-F197 (40% fatality) and Ng-F95 (100% fatality), seemed useful for revealing unknown viral determinants affecting pathogenicity in A129 mice. A reverse genetic system will be required to construct mutagenesis viruses and will provide new insights into viral genes, as demonstrated in our previous study (Wulandari et al., 2025).

Previous studies have suggested that NSs of SFTSV is a key factor in strain-specific fatality, acting as a strong interferon antagonist to suppress immune responses by interacting with key signaling molecules such as STAT1 and STAT2 and IFN-I response (Chaudhary et al., 2015; Yoshikawa et al., 2019). It has been found that critical residues in NSs, mutation of Trp_{61} to Tyr_{61}, influenced the NSs-Np interactions, which might cause conformational changes in NSs and contributed to reduced viral replication and pathogenicity of SFTSV strains (Park et al., 2023). Furthermore, mutations such as Pro_{102} to Ala_{102} and Lys_{211} to Arg_{211} influenced the NS interactions with the TPL2–ABIN2–p105 complex, promoting IL-10 production and immune suppression (Choi et al., 2019). In addition, previous studies have demonstrated that substitutions at positions 30, 144, 172, 207, 245, and 249 in the NSs of SFTSV may underlie geographic lineages and pathogenic variabilities (Wu et al., 2021). However, in this study, Thr_{172} in NSs of Yg-F197 was found in A129 mice, which are deficient in IFN-I responses. Thus, if this amino acid is related to pathogenicity, other mechanisms may be involved.

The envelope glycoproteins Gn and Gc encoded in the M segment play critical roles in viral entry and also seem to contribute to the viral pathogenesis (Hofmann et al., 2013). Previous studies, including our findings, have suggested that the Gc protein is also an important determinant of SFTSV virulence (Lei et al., 2015; Plegge et al., 2016; Wang et al., 2024; Wulandari et al., 2025). Glycosylation of viral glycoproteins has been reported to influence viral infectivity, cellular tropism, and pathogenicity, with disruption of glycan motifs associated with attenuated virulence in experimental models (Shimojima

et al., 2024). Previous studies demonstrated that loss of the Asn33-linked glycan disrupts lectin-mediated entry, reduces macrophage infection and cytokine induction, and attenuates SFTSV virulence *in vivo* (Shimojima et al., 2024). In this study, it was suggested Ile_{745} in Gc of Sh-F149, $Gly_{20,}$ and Arg_{113} in Gn, of Yg-F197 might influence the reduced virulence in A129 mice. To confirm whether these amino acids determine lower pathogenicity and elucidate the mechanism, further investigation integrating reverse genetics, structural, and functional assays will be required and will provide new insights into SFTSV pathogenicity.

SFTSV strains derived from fatal cat cases of Ng-F95, Ng-F125, Sh-F149, Yg-F180, Ng-F186, Ng-F206 and Yg-F274 showed 40% to 100% fatalities. Also, the recovered cat-derived strains of Yg-F157, Yg-F197, Ng-F265, and Yg-F267, which showed 40% to 100% fatalities in A129 mice, suggest that the pathogenicity of SFTSV strains in A129 mice is unlikely to correlate with the disease outcome of the originating cat cases, as shown in our previous study (Ando et al., 2021). All SFTSV strains except Ng-F125 were clustered within genotype J1 based on S, M, and L segments. The L segment of Ng-F125 was J3 genotype, whereas the S and M segments were J1 genotype, indicating that this strain was a reassortant virus. J1 is the predominant genotype in Japan and comprises many human and animal-derived strains from various regions (Yoshikawa et al., 2015; Ando et al., 2021). However, the varied pathogenicity in A129 mice and disease outcomes in cat cases of SFTSV strains were unlikely to be explained by large-scale genomic divergence, but rather were more likely associated with limited, strain-specific amino acid substitutions.

We previously showed that cultured susceptible cell lines, Vero E6 and TLT, exhibited high SFTSV yields, with or without CPE, respectively (Anggita et al., 2025). Thus, we considered these cells useful for examining the growth properties of SFTSV strains exhibiting different fatality rates in A129 *in vitro*. We hypothesized that highly pathogenic strains would exhibit greater propagation in cultured cells; however, there were no significant differences in growth kinetics between the two cell lines for SFTSV strains with 20-100% fatality. Our preliminary data imply that there were no significant differences in growth kinetics in other mammalian-derived cells between SFTSV strains (data not shown). Therefore, it was suggested that the replication efficiency of these SFTSV strains *in vitro* may not correlate with the pathogenicity *in vivo*. However, Vero E6 and TLT were not derived from mouse tissues, and we are proceeding to examine the virus growth in cultured cells derived from A129 mice. We aim to provide more detailed data on the mechanism of SFTSV propagation across different cell lines in the future.

3.6 Conclusion

In conclusion, this study identified several amino acid residues (Ile_{745} in Gc; Thr_{172} in NSs; Gly_{20}/Arg_{113} in Gn; and Arg_{307}/Val_{371}/Pro_{374}/Asn_{1610} in RdRp) that may attenuate SFTSV pathogenicity in A129 mice, despite all strains carrying the fatal Gly_{581}/Ser_{934} Gc pair. Comparing closely related strain pairs with divergent fatality rates provides a basis for uncovering novel virulence determinants. Thr_{172} in NSs, associated with attenuation in $IFNAR^{-/-}$ mice, suggests IFN-I-independent mechanisms. No correlation was observed between cat disease outcomes and mouse fatality, and most strains belonged to genotype J1, except the reassortant Ng-F125. In vitro growth kinetics did not reflect in vivo pathogenicity, highlighting the need for reverse genetics and mouse-derived cell lines to validate these candidate residues.

4.0 General Conclusion

The order Bunyavirales comprises one of the largest and most diverse groups of negative-sense, single-stranded RNA viruses, including emerging pathogens of significant medical and veterinary importance such as severe fever with thrombocytopenia syndrome virus (SFTSV), Rift Valley fever virus (RVFV), Hantaan virus (HNTV), and Crimean-Congo hemorrhagic fever virus (CCHFV). Bunyaviruses are typically enveloped and have a tripartite genome comprising small (S), medium (M), and large (L) segments. Many bunyaviruses are arthropod-borne (arboviruses), transmitted by mosquitoes, ticks, or sandflies, and are associated with significant human and animal diseases. Despite their public health importance, environmental stability and molecular determinants of pathogenicity vary considerably among bunyaviruses, necessitating virus-specific investigations. For SFTSV, an emerging tick-borne virus endemic to East and Southeast Asia, critical knowledge gaps remain regarding its environmental persistence and the viral factors that influence disease prognosis in vulnerable populations.

This thesis provides a comprehensive characterization of two critical aspects of SFTSV: its environmental stability across diverse temperatures and its differential pathogenicity, as revealed by amino acid substitution analysis in an $IFNAR^{-/-}$ (A129) mouse model. Regarding thermal stability, we demonstrated that SFTSV retains infectivity across a broad range from 4°C to 37°C for several days and, notably, even at near-boiling temperatures (94°C), underscoring a persistent transmission risk that warrants rigorous inactivation protocols when handling infected individuals and contaminated fomites in endemic regions. Regarding pathogenicity, we identified strain-specific amino acid substitutions associated with differential virulence in A129 mice, providing a molecular basis for understanding how limited, strain-specific changes rather than large-scale genomic divergence may influence disease outcomes in the context of Type I interferon receptor-deficient mice.

In conclusion, these findings highlight the importance of monitoring environmental conditions to shape public health strategies, combined with rigorous molecular surveillance to detect potentially attenuated or virulent strains. However, further studies are essential to fully elucidate the specific molecular mechanisms governing both the remarkable thermotolerance and the differential pathogenicity of SFTSV. Future work integrating reverse genetics, structural analyses, biophysical assays, and functional evaluations using A129 mouse-derived cells will be required to establish the mechanistic basis of these observations

Acknowledgment

First and foremost, I offer my prayerful thanks to God for all the blessings bestowed upon me throughout my life.

I would like to express my deepest gratitude to my supervisor, **Professor Daisuke HAYASAKA**, **DVM**, **PhD**, for his invaluable guidance, encouragement, and unwavering support throughout my doctoral journey. His mentorship, constructive criticism, and dedication to academic excellence have profoundly shaped my growth as a researcher and scientist. I am sincerely grateful for the opportunity to learn under his supervision.

I am also deeply thankful to **Associate Professor Hiroshi SHIMODA**, **DVM**, **PhD**, for his continued support, insightful guidance, and encouragement throughout my research and studies. His willingness to assist, share knowledge, and offer constructive advice was instrumental in the successful completion of this work. I deeply appreciate his kindness, patience, and mentorship during my time in the laboratory.

I would like to express my sincere appreciation to the following animal hospitals for providing serum and plasma samples from SFTSV-infected animals: Chitosebashi Animal Hospital, Azekari Animal Hospital, Yamashita Animal Hospital, Ohta Animal Hospital, Yunan Animal Hospital, Nakakoshi Animal Hospital, Tagawa Animal Clinic, Yoshida Animal Hospital, and Tsutsumi Animal Hospital. I also extend my gratitude to Chappie Co., Ltd. for providing Wish-s-SH for the inactivation assay. Their collaboration, cooperation, and commitment to veterinary and health research were invaluable to the successful completion of this work. I am deeply grateful for their contribution to advancing the understanding of severe fever with thrombocytopenia syndrome virus (SFTSV) infections.

My sincere thanks also go to my laboratory members and colleagues for their assistance, teamwork, stimulating discussions, and the friendly environment that made the research process both productive and enjoyable. I deeply appreciate all the support, collaboration, and shared experiences that contributed to the successful completion of this PhD.

Finally, I would like to express my heartfelt appreciation to my family, my greatest support system, for their unconditional love, prayers, patience, and continuous encouragement throughout this challenging journey. This achievement would not have been possible without you.

References

1. Allingham, C., Taniguchi, M., Kinchla, A. J., & Moore, M. D. (2024). The influence of simulated organic matter on the inactivation of viruses: A Review. *Viruses*, 16(7), 1026. https://doi.org/10.3390/v16071026
2. Ando, T., Nabeshima, T., Inoue, S., Tun, M. M. N., Obata, M., Hu, W., Shimoda, H., Kurihara, S., Izumikawa, K., Morita, K., & Hayasaka, D. (2021). Severe fever with thrombocytopenia syndrome in cats and its prevalence among veterinarian staff members in Nagasaki, Japan. *Viruses*, *13*(6), 1142. https://doi.org/10.3390/v13061142
3. Anggita, M., Nyampong, S., Hu, W., Shimoda, H., & Hayasaka, D. (2025). Different susceptibility of mammalian cell lines to severe fever with thrombocytopenia syndrome virus infection. *Viruses*, *17*(10), 1380. https://doi.org/10.3390/v17101380
4. Araújo, P. A., Lemos, M., Mergulhão, F., Melo, L., & Simões, M. (2013). The influence of interfering substances on the antimicrobial activity of selected quaternary ammonium compounds. *International journal of food science*, *2013*, 237581. https://doi.org/10.1155/2013/237581
5. Beniac, D. R., Melito, P. L., Devarennes, S. L., Hiebert, S. L., Rabb, M. J., Lamboo, L. L., Jones, S. M., & Booth, T. F. (2012). The organisation of Ebola virus reveals a capacity for extensive, modular polyploidy. *PloS one*, *7*(1), e29608. https://doi.org/10.1371/journal.pone.0029608
6. Brennan, B., Li, P., Zhang, S., Li, A., Liang, M., Li, D., & Elliott, R. M. (2015). Reverse genetics system for severe fever with thrombocytopenia syndrome virus. *Journal of virology*, *89*(6), 3026–3037. https://doi.org/10.1128/JVI.03432-14
7. Brisse, M., & Ly, H. (2019). Comparative structure and function analysis of the RIG-I-Like receptors: RIG-I and MDA5. *Frontiers in immunology*, *10*, 1586. https://doi.org/10.3389/fimmu.2019.01586
8. Bryden, S. R., Dunlop, J. I., Clarke, A. T., Fares, M., Pingen, M., Wu, Y., Willett, B. J., Patel, A. H., Gao, G. F., Kohl, A., & Brennan, B. (2022). Exploration of immunological responses underpinning severe fever with thrombocytopenia syndrome virus infection reveals IL-6 as a therapeutic target in an immunocompromised mouse model. *PNAS nexus*, *1*(1), pgac024. https://doi.org/10.1093/pnasnexus/pgac024
9. Campagna, M. V., Faure-Kumar, E., Treger, J. A., Cushman, J. D., Grogan, T. R., Kasahara, N., & Lawson, G. W. (2016). Factors in the selection of surface disinfectants for use in a laboratory animal setting. *Journal of the American Association for Laboratory Animal Science: JAALAS*, *55*(2), 175–188.

10. Chaudhary, V., Zhang, S., Yuen, K. S., Li, C., Lui, P. Y., Fung, S. Y., Wang, P. H., Chan, C. P., Li, D., Kok, K. H., Liang, M., & Jin, D. Y. (2015). Suppression of type I and type III IFN signalling by NSs protein of severe fever with thrombocytopenia syndrome virus through inhibition of STAT1 phosphorylation and activation. *The Journal of general virology*, *96*(11), 3204–3211. https://doi.org/10.1099/jgv.0.000280
11. Choi, Y., Park, S. J., Sun, Y., Yoo, J. S., Pudupakam, R. S., Foo, S. S., Shin, W. J., Chen, S. B., Tsichlis, P. N., Lee, W. J., Lee, J. S., Li, W., Brennan, B., Choi, Y. K., & Jung, J. U. (2019). Severe fever with thrombocytopenia syndrome phlebovirus non-structural protein activates TPL2 signalling pathway for viral immunopathogenesis. *Nature microbiology*, *4*(3), 429–437. https://doi.org/10.1038/s41564-018-0329-x
12. Christensen, J. and Linden, K.G. (2003). How particles affect UV light in the UV disinfection of unfiltered drinking water. *Journal - American Water Works Association*, 95: 179–189. https://doi.org/10.1002/j.1551-8833.2003.tb10344.x
13. Cutts, T. A., Robertson, C., Theriault, S. S., Nims, R. W., Kasloff, S. B., Rubino, J. R., & Ijaz, M. K. (2020). Efficacy of microbicides for inactivation of Ebola-Makona virus on a non-porous surface: a targeted hygiene intervention for reducing virus spread. *Scientific reports*, *10*(1), 15247. https://doi.org/10.1038/s41598-020-71736-x
14. Dalskov, L., Gad, H. H., & Hartmann, R. (2023). Viral recognition and the antiviral interferon response. *The EMBO journal*, *42*(14), e112907. https://doi.org/10.15252/embj.2022112907
15. Darnell, M. E., Subbarao, K., Feinstone, S. M., & Taylor, D. R. (2004). Inactivation of the coronavirus that induces severe acute respiratory syndrome, SARS-CoV. *Journal of virological methods*, *121*(1), 85–91. https://doi.org/10.1016/j.jviromet.2004.06.006
16. Ding, S., Yin, H., Xu, X., Liu, G., Jiang, S., Wang, W., Han, X., Liu, J., Niu, G., Zhang, X., Yu, X. J., & Wang, X. (2014). A cross-sectional survey of severe fever with thrombocytopenia syndrome virus infection of domestic animals in Laizhou City, Shandong Province, China. *Japanese journal of infectious diseases*, *67*(1), 1–4. https://doi.org/10.7883/yoken.67.1
17. Du, S., Peng, R., Xu, W., Qu, X., Wang, Y., Wang, J., Li, L., Tian, M., Guan, Y., Wang, J., Wang, G., Li, H., Deng, L., Shi, X., Ma, Y., Liu, F., Sun, M., Wei, Z., Jin, N., Liu, W., … Li, C. (2023). Cryo-EM structure of severe fever with thrombocytopenia syndrome virus. *Nature communications*, *14*(1), 6333. https://doi.org/10.1038/s41467-023-41804-7
18. Duffy S. (2018). Why are RNA virus mutation rates so damn high? *PLoS biology*, *16*(8), e3000003. https://doi.org/10.1371/journal.pbio.3000003

19. Elliott R. M. (2014). Orthobunyaviruses: recent genetic and structural insights. *Nature reviews. Microbiology*, *12*(10), 673–685. https://doi.org/10.1038/nrmicro3332

20. Fang, X., Hu, J., Peng, Z., Dai, Q., Liu, W., Liang, S., Li, Z., Zhang, N., & Bao, C. (2021). Epidemiological and clinical characteristics of severe fever with thrombocytopenia syndrome bunyavirus human-to-human transmission. *PLoS neglected tropical diseases*, *15*(4), e0009037. https://doi.org/10.1371/journal.pntd.0009037

21. Freiberg, A. N., Sherman, M. B., Morais, M. C., Holbrook, M. R., & Watowich, S. J. (2008). Three-dimensional organization of Rift Valley fever virus revealed by cryoelectron tomography. *Journal of virology*, *82*(21), 10341–10348. https://doi.org/10.1128/JVI.01191-08

22. Friedler, E., F. Chavez, D., Alfiya, Y., Gilboa, Y., & Gross, A. (2021). impact of suspended solids and organic matter on chlorine and uv disinfection efficiency of greywater. *Water*, *13*(2), 214. https://doi.org/10.3390/w13020214

23. Gai, Z., Liang, M., Zhang, Y., Zhang, S., Jin, C., Wang, S. W., Sun, L., Zhou, N., Zhang, Q., Sun, Y., Ding, S. J., Li, C., Gu, W., Zhang, F., Wang, Y., Bian, P., Li, X., Wang, Z., Song, X., Wang, X., … Li, D. (2012). Person-to-person transmission of severe fever with thrombocytopenia syndrome bunyavirus through blood contact. *Clinical infectious diseases: an official publication of the Infectious Diseases Society of America*, *54*(2), 249–252. https://doi.org/10.1093/cid/cir776

24. Halldorsson, S., Behrens, A. J., Harlos, K., Huiskonen, J. T., Elliott, R. M., Crispin, M., Brennan, B., & Bowden, T. A. (2016). Structure of a phleboviral envelope glycoprotein reveals a consolidated model of membrane fusion. *Proceedings of the National Academy of Sciences of the United States of America*, *113*(26), 7154–7159. https://doi.org/10.1073/pnas.1603827113

25. Halldorsson, S., Li, S., Li, M., Harlos, K., Bowden, T. A., & Huiskonen, J. T. (2018). Shielding and activation of a viral membrane fusion protein. *Nature communications*, *9*(1), 349. https://doi.org/10.1038/s41467-017-02789-2

26. Harada, T., Fukushi, S., Kurosu, T., Yoshikawa, T., Shimojima, M., Tanabayashi, K., & Saijo, M. (2020). Inactivation of severe fever with thrombocytopenia syndrome virus for improved laboratory safety. Journal of Biosafety and Biosecurity, 2(1), 31–35. https://doi.org/10.1016/j.jobb.2020.03.001

27. Hayasaka, D., Shimada, S., Aoki, K., Takamatsu, Y., Uchida, L., Horio, M., Fuxun, Y., & Morita, K. (2015). epidemiological survey of severe fever with thrombocytopenia syndrome virus in ticks in nagasaki, japan. *Tropical medicine and health*, *43*(3), 159–164. https://doi.org/10.2149/tmh.2015-01

28. Hofmann, H., Li, X., Zhang, X., Liu, W., Kühl, A., Kaup, F., Soldan, S. S., González-Scarano, F., Weber, F., He, Y., & Pöhlmann, S. (2013). Severe fever with thrombocytopenia virus glycoproteins are targeted by neutralizing

antibodies and can use DC-SIGN as a receptor for pH-dependent entry into human and animal cell lines. *Journal of virology*, *87*(8), 4384–4394. https://doi.org/10.1128/JVI.02628-12

29. Hu, W., Shimoda, H., Tsuchiya, Y., Kishi, M., & Hayasaka, D. (2024). pH-dependent virucidal effects of weak acids against pathogenic viruses. *Tropical medicine and health*, 52(1), 9. https://doi.org/10.1186/s41182-023-00573-1
30. Jiao, L., Duyang, S., Liang, M., Niu, F., Shaw, N., Wu, W., Ding, W., Jin, C., Peng, Y., Zhu, Y., Zhang, F., Wang, T., Li, C., Zuo, X., Luan, C. H., Li, D., & Liu, Z. J. (2013). Structure of severe fever with thrombocytopenia syndrome virus nucleocapsid protein in complex with suramin reveals therapeutic potential. *Journal of Virology*, 87(12), 6829–6839. https://doi.org/10.1128/JVI.00373-13
31. Jin, C., Liang, M., Ning, J., Gu, W., Jiang, H., Wu, W., Zhang, F., Li, C., Zhang, Q., Zhu, H., Chen, T., Han, Y., Zhang, W., Zhang, S., Wang, Q., Sun, L., Liu, Q., Li, J., Wang, T., Wei, Q., … Li, D. (2012). Pathogenesis of emerging severe fever with thrombocytopenia syndrome virus in C57/BL6 mouse model. *Proceedings of the National Academy of Sciences of the United States of America*, *109*(25), 10053–10058. https://doi.org/10.1073/pnas.1120246109
32. Jones, K. E., Patel, N. G., Levy, M. A., Storeygard, A., Balk, D., Gittleman, J. L., & Daszak, P. (2008). Global trends in emerging infectious diseases. *Nature*, *451*(7181), 990–993. https://doi.org/10.1038/nature06536
33. Kalyaanamoorthy, S., Minh, B. Q., Wong, T. K. F., von Haeseler, A., & Jermiin, L. S. (2017). ModelFinder: fast model selection for accurate phylogenetic estimates. *Nature methods*, *14*(6), 587–589. https://doi.org/10.1038/nmeth.4285
34. Kampf, G., Todt, D., Pfaender, S., & Steinmann, E. (2020). Persistence of coronaviruses on inanimate surfaces and their inactivation with biocidal agents. *The Journal of hospital infection*, *104*(3), 246–251. https://doi.org/10.1016/j.jhin.2020.01.022
35. Kaneko, C., Saito, A., Inagaki, H., Sugiyama, H., Mazimpaka, E., Fujimoto, S., & Okabayashi, T. (2022). Rapid inactivation of Dabie bandavirus (SFTSV) by irradiation with deep-ultraviolet light-emitting diode. *Journal of medical virology*, *94*(7), 3438–3441. https://doi.org/10.1002/jmv.27698
36. Kida, K., Matsuoka, Y., Shimoda, T., Matsuoka, H., Yamada, H., Saito, T., Imataki, O., Kadowaki, N., Noguchi, K., Maeda, K., Mochizuki, Y., & Kishimoto, T. (2019). A case of cat-to-human transmission of severe fever with thrombocytopenia syndrome virus. *Japanese journal of infectious diseases*, *72*(5), 356–358. https://doi.org/10.7883/yoken.JJID.2018.526

37. Kim, K. H., Kim, J., Ko, M., Chun, J. Y., Kim, H., Kim, S., Min, J. Y., Park, W. B., Oh, M. D., & Chung, J. (2019). An anti-Gn glycoprotein antibody from a convalescent patient potently inhibits the infection of severe fever with thrombocytopenia syndrome virus. *PLoS pathogens*, *15*(2), e1007375. https://doi.org/10.1371/journal.ppat.1007375

38. Kim, K. H., Yi, J., Kim, G., Choi, S. J., Jun, K. I., Kim, N. H., Choe, P. G., Kim, N. J., Lee, J. K., & Oh, M. D. (2013). Severe fever with thrombocytopenia syndrome, South Korea, 2012. *Emerging infectious diseases*, *19*(11), 1892–1894. https://doi.org/10.3201/eid1911.130792

39. Kim, Y. R., Yun, Y., Bae, S. G., Park, D., Kim, S., Lee, J. M., Cho, N. H., Kim, Y. S., & Lee, K. H. (2018). Severe Fever with Thrombocytopenia Syndrome Virus Infection, South Korea, 2010. *Emerging infectious diseases*, *24*(11), 2103–2105. https://doi.org/10.3201/eid2411.170756

40. Kirino, Y., Ishijima, K., Miura, M., Nomachi, T., Mazimpaka, E., Sudaryatma, P. E., Yamanaka, A., Maeda, K., Sugimoto, T., Saito, A., Mekata, H., & Okabayashi, T. (2021). Seroprevalence of severe fever with thrombocytopenia syndrome virus in small animal veterinarians and nurses in the Japanese prefecture with the highest case load. *Viruses*, 13(2), 229. https://doi.org/10.3390/v13020229

41. Kopitar-Jerala N. (2017). The role of interferons in inflammation and inflammasome activation. *Frontiers in immunology*, *8*, 873. https://doi.org/10.3389/fimmu.2017.00873

42. Kuwata, R., Sugiyama, H., Yonemitsu, K., Van Dung, N., Terada, Y., Taniguchi, M., Shimoda, H., Takano, A., & Maeda, K. (2015). Isolation of Japanese encephalitis virus and a novel insect-specific flavivirus from mosquitoes collected in a cowshed in Japan. *Archives of virology*, *160*(9), 2151–2159. https://doi.org/10.1007/s00705-015-2488-x

43. Lee, J. K., & Shin, O. S. (2021). Nonstructural protein of severe fever with thrombocytopenia syndrome phlebovirus inhibits tbk1 to evade interferon-mediated response. *Journal of microbiology and biotechnology*, *31*(2), 226–232. https://doi.org/10.4014/jmb.2008.08048

44. Lei, X. Y., Liu, M. M., & Yu, X. J. (2015). Severe fever with thrombocytopenia syndrome and its pathogen SFTSV. *Microbes and infection*, *17*(2), 149–154. https://doi.org/10.1016/j.micinf.2014.12.002

45. Li, J., Wang, C., Li, X., Zhang, G., Sun, S., Wang, Z., Zhao, J., Xiu, L., Jiang, N., Zhang, H., Yang, Z., & Zhang, J. (2024). Direct transmission of severe fever with thrombocytopenia syndrome virus from farm-raised fur animals to workers in Weihai, China. *Virology journal*, *21*(1), 113. https://doi.org/10.1186/s12985-024-02387-x

46. Lin, T. L., Ou, S. C., Maeda, K., Shimoda, H., Chan, J. P., Tu, W. C., Hsu, W. L., & Chou, C. C. (2020). The first discovery of severe fever with thrombocytopenia syndrome virus in Taiwan. *Emerging microbes & infections*, *9*(1), 148–151. https://doi.org/10.1080/22221751.2019.1710436

47. Liu, J. W., Zhao, L., Luo, L. M., Liu, M. M., Sun, Y., Su, X., & Yu, X. J. (2016). Molecular evolution and spatial transmission of severe fever with thrombocytopenia syndrome virus based on complete genome sequences. *PloS one*, *11*(3), e0151677. https://doi.org/10.1371/journal.pone.0151677

48. Liu, Q., He, B., Huang, S. Y., Wei, F., & Zhu, X. Q. (2014). Severe fever with thrombocytopenia syndrome, an emerging tick-borne zoonosis. *The Lancet. Infectious diseases*, *14*(8), 763–772. https://doi.org/10.1016/S1473-3099(14)70718-2

49. Liu, Y., Wu, B., Paessler, S., Walker, D. H., Tesh, R. B., & Yu, X. J. (2014). The pathogenesis of severe fever with thrombocytopenia syndrome virus infection in alpha/beta interferon knockout mice: insights into the pathologic mechanisms of a new viral hemorrhagic fever. *Journal of virology*, *88*(3), 1781–1786. https://doi.org/10.1128/JVI.02277-13

50. Lokupathirage, S. M. W., Tsuda, Y., Ikegame, K., Noda, K., Muthusinghe, D. S., Kozawa, F., Manzoor, R., Shimizu, K., & Yoshimatsu, K. (2021). Subcellular localization of nucleocapsid protein of SFTSV and its assembly into the ribonucleoprotein complex with L protein and viral RNA. *Scientific reports*, *11*(1), 22977. https://doi.org/10.1038/s41598-021-01985-x

51. Lundu, T., Tsuda, Y., Ito, R., Shimizu, K., Kobayashi, S., Yoshii, K., Yoshimatsu, K., Arikawa, J., & Kariwa, H. (2018). Targeting of severe fever with thrombocytopenia syndrome virus structural proteins to the ERGIC (endoplasmic reticulum Golgi intermediate compartment) and Golgi complex. *Biomedical research (Tokyo, Japan)*, *39*(1), 27–38. https://doi.org/10.2220/biomedres.39.27

52. Lv, Q., Zhang, H., Tian, L., Zhang, R., Zhang, Z., Li, J., Tong, Y., Fan, H., Carr, M. J., & Shi, W. (2017). Novel sub-lineages, recombinants and reassortants of severe fever with thrombocytopenia syndrome virus. *Ticks and tick-borne diseases*, *8*(3), 385–390. https://doi.org/10.1016/j.ttbdis.2016.12.015

53. Matsuno, K., Nonoue, N., Noda, A., Kasajima, N., Noguchi, K., Takano, A., Shimoda, H., Orba, Y., Muramatsu, M., Sakoda, Y., Takada, A., Minami, S., Une, Y., Morikawa, S., & Maeda, K. (2018). Fatal tickborne phlebovirus infection in captive cheetahs, Japan. *Emerging infectious diseases*, *24*(9), 1726–1729. https://doi.org/10.3201/eid2409.171667

54. Matsuno, K., Orba, Y., Maede-White, K., Scott, D., Feldmann, F., Liang, M., & Ebihara, H. (2017). Animal models of emerging tick-borne phleboviruses: determining target cells in a lethal model of sftsv infection. *Frontiers in microbiology*, 8, 104. https://doi.org/10.3389/fmicb.2017.00104

55. Matsuu, A., Momoi, Y., Nishiguchi, A., Noguchi, K., Yabuki, M., Hamakubo, E., Take, M., & Maeda, K. (2019). Natural severe fever with thrombocytopenia syndrome virus infection in domestic cats in Japan. *Veterinary microbiology*, *236*, 108346. https://doi.org/10.1016/j.vetmic.2019.06.019

56. Minh, B. Q., Schmidt, H. A., Chernomor, O., Schrempf, D., Woodhams, M. D., von Haeseler, A., & Lanfear, R. (2020). IQ-TREE 2: new models and efficient methods for phylogenetic inference in the genomic era. *Molecular biology and evolution*, *37*(5), 1530–1534. https://doi.org/10.1093/molbev/msaa015

57. Morens, D. M., Folkers, G. K., & Fauci, A. S. (2004). The challenge of emerging and re-emerging infectious diseases. *Nature*, *430*(6996), 242–249. https://doi.org/10.1038/nature02759

58. Müller, U., Steinhoff, U., Reis, L. F., Hemmi, S., Pavlovic, J., Zinkernagel, R. M., & Aguet, M. (1994). Functional role of type I and type II interferons in antiviral defense. *Science (New York, N.Y.)*, *264*(5167), 1918–1921. https://doi.org/10.1126/science.8009221

59. Ning, Y. J., Feng, K., Min, Y. Q., Cao, W. C., Wang, M., Deng, F., Hu, Z., & Wang, H. (2015). Disruption of type I interferon signaling by the nonstructural protein of severe fever with thrombocytopenia syndrome virus via the hijacking of STAT2 and STAT1 into inclusion bodies. *Journal of virology*, *89*(8), 4227–4236. https://doi.org/10.1128/JVI.00154-15

60. Ning, Y. J., Wang, M., Deng, M., Shen, S., Liu, W., Cao, W. C., Deng, F., Wang, Y. Y., Hu, Z., & Wang, H. (2014). Viral suppression of innate immunity via spatial isolation of TBK1/IKKε from mitochondrial antiviral platform. *Journal of molecular cell biology*, *6*(4), 324–337. https://doi.org/10.1093/jmcb/mju015

61. Niu, G., Li, J., Liang, M., Jiang, X., Jiang, M., Yin, H., Wang, Z., Li, C., Zhang, Q., Jin, C., Wang, X., Ding, S., Xing, Z., Wang, S., Bi, Z., & Li, D. (2013). Severe fever with thrombocytopenia syndrome virus among domesticated animals, China. *Emerging infectious diseases*, *19*(5), 756–763. https://doi.org/10.3201/eid1905.120245

62. Overby, A. K., Pettersson, R. F., & Neve, E. P. (2007). The glycoprotein cytoplasmic tail of Uukuniemi virus (Bunyaviridae) interacts with ribonucleoproteins and is critical for genome packaging. *Journal of virology*, *81*(7), 3198–3205. https://doi.org/10.1128/JVI.02655-06

63. Palma, F., Díaz-Navarro, M., Visedo, A., Sanz-Ruíz, P., Brandi, G., Schiavano, G. F., & Guembe, M. (2025). Assessment of the anti-biofilm effect of UV-C irradiation (254 nm) against healthcare associated infections related microorganisms. *Frontiers in microbiology*, *16*, 1570334. https://doi.org/10.3389/fmicb.2025.1570334

64. Park, D., Kim, K. W., Kim, Y. I., Casel, M. A. B., Jang, H., Kwon, W., Kim, K., Kim, S. M., N, M. P. A., Kim, E. H., Jang, H., Hwang, S., Yun, S. M., Lee, J. Y., Jeong, H. W., Park, S. J., & Choi, Y. K. (2024). Deciphering the evolutionary landscape of severe fever with thrombocytopenia syndrome virus across East Asia. *Virus evolution*, *10*(1), veae054. https://doi.org/10.1093/ve/veae054

65. Park, E. S., Shimojima, M., Nagata, N., Ami, Y., Yoshikawa, T., Iwata-Yoshikawa, N., Fukushi, S., Watanabe, S., Kurosu, T., Kataoka, M., Okutani, A., Kimura, M., Imaoka, K., Hanaki, K., Suzuki, T., Hasegawa, H., Saijo, M., Maeda, K., & Morikawa, S. (2019). Severe fever with thrombocytopenia syndrome phlebovirus causes lethal viral hemorrhagic fever in cats. *Scientific reports*, *9*(1), 11990. https://doi.org/10.1038/s41598-019-48317-8

66. Park, J. Y., Sivasankar, C., Kirthika, P., Prabhu, D., & Lee, J. H. (2023). Non-structural protein-w61 as a novel target in severe fever with thrombocytopenia syndrome virus (SFTSV): An in-vitro and in-silico study on protein-protein interactions with nucleoprotein and viral replication. *Viruses*, *15*(9), 1963. https://doi.org/10.3390/v15091963

67. Piercy, T. J., Smither, S. J., Steward, J. A., Eastaugh, L., & Lever, M. S. (2010). The survival of filoviruses in liquids, on solid substrates and in a dynamic aerosol. *Journal of applied microbiology*, *109*(5), 1531–1539. https://doi.org/10.1111/j.1365-2672.2010.04778.x

68. Plegge, T., Hofmann-Winkler, H., Spiegel, M., & Pöhlmann, S. (2016). evidence that processing of the severe fever with thrombocytopenia syndrome virus gn/gc polyprotein is critical for viral infectivity and requires an internal gc signal peptide. *PloS one*, *11*(11), e0166013. https://doi.org/10.1371/journal.pone.0166013

69. Rabenau, H. F., Cinatl, J., Morgenstern, B., Bauer, G., Preiser, W., & Doerr, H. W. (2005). Stability and inactivation of SARS coronavirus. *Medical microbiology and immunology*, *194*(1-2), 1–6. https://doi.org/10.1007/s00430-004-0219-0

70. Rahn, R. O., Stefan, M. I., Bolton, J. R., Goren, E., Shaw, P. S., & Lykke, K. R. (2003). Quantum yield of the iodide-iodate chemical actinometer: dependence on wavelength and concentrations. *Photochemistry and photobiology*, *78*(2), 146–152. https://doi.org/10.1562/0031-8655(2003)078<0146:qyotic>2.0.co;2

71. Reguera, J., Gerlach, P., Rosenthal, M., Gaudon, S., Coscia, F., Günther, S., & Cusack, S. (2016). Comparative structural and functional analysis of bunyavirus and arenavirus cap-snatching endonucleases. *PLoS pathogens*, *12*(6), e1005636. https://doi.org/10.1371/journal.ppat.1005636

72. Rutala, W. A., & Weber, D. J. (2008). Guideline for disinfection and sterilization in healthcare facilities. Centers for Disease Control and Prevention.

73. Sakai, Y., Kuwabara, Y., Ishijima, K., Kagimoto, S., Mura, S., Tatemoto, K., Kuwata, R., Yonemitsu, K., Minami, S., Kuroda, Y., Baba, K., Okuda, M., Shimoda, H., Sakurai, M., Morimoto, M., & Maeda, K. (2021). Histopathological characterization of cases of spontaneous fatal feline severe fever with thrombocytopenia syndrome, Japan. *Emerging infectious diseases*, *27*(4), 1068–1076. https://doi.org/10.3201/eid2704.204148

74. Shimada, S., Posadas-Herrera, G., Aoki, K., Morita, K., & Hayasaka, D. (2015). Therapeutic effect of post-exposure treatment with antiserum on severe fever with thrombocytopenia syndrome (SFTS) in a mouse model of SFTS virus infection. *Virology*, *482*, 19–27. https://doi.org/10.1016/j.virol.2015.03.010

75. Shimoda, H., Matsuda, J., Iwasaki, T., & Hayasaka, D. (2021). Efficacy of 265-nm ultraviolet light in inactivating infectious SARS-CoV-2. *Journal of photochemistry and photobiology*, *7*, 100050. https://doi.org/10.1016/j.jpap.2021.100050

76. Shimojima, M., Sugimoto, S., Taniguchi, S., Maeki, T., Yoshikawa, T., Kurosu, T., Tajima, S., Lim, C. K., & Ebihara, H. (2024). N-glycosylation of viral glycoprotein is a novel determinant for the tropism and virulence of highly pathogenic tick-borne bunyaviruses. *PLoS pathogens*, *20*(7), e1012348. https://doi.org/10.1371/journal.ppat.1012348

77. Song, H., Li, J., Shi, S., Yan, L., Zhuang, H., & Li, K. (2010). Thermal stability and inactivation of hepatitis C virus grown in cell culture. *Virology journal*, *7*, 40. https://doi.org/10.1186/1743-422X-7-40

78. Sun, J. M., Wu, H. X., Lu, L., Liu, Y., Mao, Z. Y., Ren, J. P., Yao, W. W., Qu, H. H., & Liu, Q. Y. (2021). Factors associated with spatial distribution of severe fever with thrombocytopenia syndrome. *The Science of the total environment*, *750*, 141522. https://doi.org/10.1016/j.scitotenv.2020.141522

79. Sun, Y., Jin, C., Zhan, F., Wang, X., Liang, M., Zhang, Q., Ding, S., Guan, X., Huo, X., Li, C., Qu, J., Wang, Q., Zhang, S., Zhang, Y., Wang, S., Xu, A., Bi, Z., & Li, D. (2012). Host cytokine storm is associated with disease severity of severe fever with thrombocytopenia syndrome. *The Journal of infectious diseases*, *206*(7), 1085–1094. https://doi.org/10.1093/infdis/jis452

80. Tabara, K., Fujita, H., Hirata, A., & Hayasaka, D. (2016). Investigation of severe fever with thrombocytopenia syndrome virus antibody among domestic bovines transported to slaughterhouse in Shimane Prefecture, Japan. *Japanese journal of infectious diseases*, *69*(5), 445–447. https://doi.org/10.7883/yoken.JJID.2015.624

81. Takahashi, T., Maeda, K., Suzuki, T., Ishido, A., Shigeoka, T., Tominaga, T., Kamei, T., Honda, M., Ninomiya, D., Sakai, T., Senba, T., Kaneyuki, S., Sakaguchi, S., Satoh, A., Hosokawa, T., Kawabe, Y., Kurihara, S., Izumikawa,

K., Kohno, S., Azuma, T., … Saijo, M. (2014). The first identification and retrospective study of Severe Fever with Thrombocytopenia Syndrome in Japan. *The Journal of infectious diseases*, *209*(6), 816–827. https://doi.org/10.1093/infdis/jit603

82. Tani, H., Fukuma, A., Fukushi, S., Taniguchi, S., Yoshikawa, T., Iwata-Yoshikawa, N., Sato, Y., Suzuki, T., Nagata, N., Hasegawa, H., Kawai, Y., Uda, A., Morikawa, S., Shimojima, M., Watanabe, H., & Saijo, M. (2016). Efficacy of T-705 (Favipiravir) in the treatment of infections with lethal severe fever with thrombocytopenia syndrome virus. *mSphere*, *1*(1), e00061-15. https://doi.org/10.1128/mSphere.00061-15
83. Tani, H., Kawachi, K., Kimura, M., Taniguchi, S., Shimojima, M., Fukushi, S., Igarashi, M., Morikawa, S., & Saijo, M. (2019). Identification of the amino acid residue important for fusion of severe fever with thrombocytopenia syndrome virus glycoprotein. Virology, 535, 102–110. https://doi.org/10.1016/j.virol.2019.06.014
84. Tran, X. C., Yun, Y., Van An, L., Kim, S. H., Thao, N. T. P., Man, P. K. C., Yoo, J. R., Heo, S. T., Cho, N. H., & Lee, K. H. (2019). Endemic severe fever with thrombocytopenia syndrome, Vietnam. *Emerging infectious diseases*, *25*(5), 1029–1031. https://doi.org/10.3201/eid2505.181463
85. Tsuru, M., Suzuki, T., Murakami, T., Matsui, K., Maeda, Y., Yoshikawa, T., Kurosu, T., Shimojima, M., Shimada, T., Hasegawa, H., Maeda, K., Morikawa, S., & Saijo, M. (2021). Pathological characteristics of a patient with severe fever with thrombocytopenia syndrome (SFTS) infected with SFTS virus through a sick cat's bite. *Viruses*, *13*(2), 204. https://doi.org/10.3390/v13020204
86. Uckeley, Z. M., Duboeuf, M., Gu, Y., Erny, A., Mazelier, M., Lüchtenborg, C., Winter, S. L., Schad, P., Mathieu, C., Koch, J., Boulant, S., Chlanda, P., Maisse, C., Brügger, B., & Lozach, P. Y. (2024). Glucosylceramide in bunyavirus particles is essential for virus binding to host cells. *Cellular and molecular life sciences: CMLS*, *81*(1), 71. https://doi.org/10.1007/s00018-023-05103-0
87. Walter, C. T., & Barr, J. N. (2011). Recent advances in the molecular and cellular biology of bunyaviruses. *The Journal of general virology*, *92*(Pt 11), 2467–2484. https://doi.org/10.1099/vir.0.035105-0
88. Wang, B., Zhang, L., Deng, F., Hu, Z., Wang, M., & Liu, J. (2024). Hsp90 β is critical for the infection of severe fever with thrombocytopenia syndrome virus. *Virologica Sinica*, *39*(1), 113–122. https://doi.org/10.1016/j.virs.2023.11.008
89. Wang, Y., Pang, B., Wang, Z., Tian, X., Xu, X., Chong, X., Liang, H., Ma, W., Kou, Z., & Wen, H. (2023). Genomic diversity and evolution analysis of severe fever with thrombocytopenia syndrome in East Asia from 2010 to 2022. *Frontiers in microbiology*, *14*, 1233693. https://doi.org/10.3389/fmicb.2023.1233693

90. World Health Organization. (2018). R&D blueprint: List of priority diseases. Retrieved May 10, 2026, from https://www.who.int/activities/prioritizing-diseases-for-research-and-development

91. Wu, X., Li, M., Zhang, Y., Liang, B., Shi, J., Fang, Y., Su, Z., Li, M., Zhang, W., Xu, L., Wang, J., Wu, Q., Tang, S., Wang, H., Zhang, T., Peng, C., Zheng, X., Deng, F., & Shen, S. (2021). Novel SFTSV Phylogeny Reveals New Reassortment Events and Migration Routes. *Virologica Sinica*, *36*(2), 300–310. https://doi.org/10.1007/s12250-020-00289-0

92. Wu, X., Qi, X., Qu, B., Zhang, Z., Liang, M., Li, C., Cardona, C. J., Li, D., & Xing, Z. (2014). Evasion of antiviral immunity through sequestering of TBK1/IKKε/IRF3 into viral inclusion bodies. *Journal of Virology*, 88(6), 3067–3076. https://doi.org/10.1128/JVI.03510-13

93. Wulandari, S., Nyampong, S., Beránková, M., Lokupathirage, S. M. W., Yoshimatsu, K., Shimoda, H., & Hayasaka, D. (2025). Two amino acid pairs in the Gc glycoprotein of severe fever with thrombocytopenia syndrome virus responsible for the enhanced virulence. *Virology*, *601*, 110294. https://doi.org/10.1016/j.virol.2024.110294

94. Xing, C., Zhang, C., Xu, Z., Wang, Y., Lu, W., Liu, X., Zhang, Y., Ma, J., Yang, S., Du, Y., Xu, G., & Liu, Y. (2025). Genome-wide CRISPR screening identifies LRP1 as an entry factor for SFTSV. *Nature communications*, *16*(1), 4036. https://doi.org/10.1038/s41467-025-59305-0

95. Xu, D. L., Zhang, X. M., Tian, X. Y., Wang, X. J., Zhao, L., Gao, M. Y., Li, L. F., Zhao, J. Q., Cao, W. C., & Ding, S. J. (2024). Changes in cytokine levels in patients with severe fever with thrombocytopenia syndrome virus. *Journal of inflammation research*, *17*, 211–222. https://doi.org/10.2147/JIR.S444398

96. Yamanaka, A., Kirino, Y., Fujimoto, S., Ueda, N., Himeji, D., Miura, M., Sudaryatma, P. E., Sato, Y., Tanaka, H., Mekata, H., & Okabayashi, T. (2020). direct transmission of severe fever with thrombocytopenia syndrome virus from domestic cat to veterinary personnel. *Emerging infectious diseases*, *26*(12), 2994–2998. https://doi.org/10.3201/eid2612.191513

97. Yan, J. M., Zhang, W. K., Yan, L. N., Jiao, Y. J., Zhou, C. M., & Yu, X. J. (2022). Bunyavirus SFTSV exploits autophagic flux for viral assembly and egress. Autophagy, 18(7), 1599–1612. https://doi.org/10.1080/15548627.2021.1994296

98. Yoshikawa, R., Kawakami, M., & Yasuda, J. (2023). The NSs protein of severe fever with thrombocytopenia syndrome virus differentially inhibits the type 1 interferon response among animal species. *The Journal of biological chemistry*, *299*(6), 104819. https://doi.org/10.1016/j.jbc.2023.104819

99. Yoshikawa, R., Sakabe, S., Urata, S., & Yasuda, J. (2019). Species-specific pathogenicity of severe fever with thrombocytopenia syndrome virus is determined by Anti-STAT2 activity of NSs. *Journal of virology*, *93*(10), e02226-18. https://doi.org/10.1128/JVI.02226-18

100. Yoshikawa, T., Shimojima, M., Fukushi, S., Tani, H., Fukuma, A., Taniguchi, S., Singh, H., Suda, Y., Shirabe, K., Toda, S., Shimazu, Y., Nomachi, T., Gokuden, M., Morimitsu, T., Ando, K., Yoshikawa, A., Kan, M., Uramoto, M., Osako, H., Kida, K., … Saijo, M. (2015). Phylogenetic and Geographic Relationships of Severe Fever with Thrombocytopenia Syndrome Virus in China, South Korea, and Japan. *The Journal of infectious diseases*, 212(6), 889–898. https://doi.org/10.1093/infdis/jiv144

101. Yu, X. J., Liang, M. F., Zhang, S. Y., Liu, Y., Li, J. D., Sun, Y. L., Zhang, L., Zhang, Q. F., Popov, V. L., Li, C., Qu, J., Li, Q., Zhang, Y. P., Hai, R., Wu, W., Wang, Q., Zhan, F. X., Wang, X. J., Kan, B., Wang, S. W., … Li, D. X. (2011). Fever with thrombocytopenia associated with a novel bunyavirus in China. *The New England journal of medicine*, *364*(16), 1523–1532. https://doi.org/10.1056/NEJMoa1010095

102. Yun, S. M., Lee, W. G., Ryou, J., Yang, S. C., Park, S. W., Roh, J. Y., Lee, Y. J., Park, C., & Han, M. G. (2014). Severe fever with thrombocytopenia syndrome virus in ticks collected from humans, South Korea, 2013. *Emerging infectious diseases*, *20*(8), 1358–1361. https://doi.org/10.3201/eid2008.131857

103. Zhang, Y. Z., Zhou, D. J., Qin, X. C., Tian, J. H., Xiong, Y., Wang, J. B., Chen, X. P., Gao, D. Y., He, Y. W., Jin, D., Sun, Q., Guo, W. P., Wang, W., Yu, B., Li, J., Dai, Y. A., Li, W., Peng, J. S., Zhang, G. B., Zhang, S., … Xu, J. (2012). The ecology, genetic diversity, and phylogeny of Huaiyangshan virus in China. *Journal of virology*, *86*(5), 2864–2868. https://doi.org/10.1128/JVI.06192-11

104. Zhang, Y. Z., Zhou, D. J., Xiong, Y., Chen, X. P., He, Y. W., Sun, Q., Yu, B., Li, J., Dai, Y. A., Tian, J. H., Qin, X. C., Jin, D., Cui, Z., Luo, X. L., Li, W., Lu, S., Wang, W., Peng, J. S., Guo, W. P., Li, M. H., … Xu, J. (2011). Hemorrhagic fever caused by a novel tick-borne Bunyavirus in Huaiyangshan, China. *Zhonghua liu xing bing xue*, *32*(3), 209–220.

105. Zhou, H., Sun, Y., Wang, Y., Liu, M., Liu, C., Wang, W., Liu, X., Li, L., Deng, F., Wang, H., Guo, Y., & Lou, Z. (2013). The nucleoprotein of severe fever with thrombocytopenia syndrome virus processes a stable hexameric ring to facilitate RNA encapsidation. *Protein & cell*, *4*(6), 445–455. https://doi.org/10.1007/s13238-013-3901-4